USE OF MOTION ARTIFACT FOR THE DETECTION OF RESPIRATORY EFFORT IN POLYSOMNOGRAPHY

A Thesis

Presented to

the Faculty of the Department of Biomedical Engineering

University of Houston

In Partial Fulfillment

of the Requirements for the Degree

Master of Science

In Biomedical Engineering

by

Jatin Tekchandani

December 2018

USE OF MOTION ARTIFACT FOR THE DETECTION OF RESPIRATORY EFFORT IN POLYSOMNOGRAPHY

_____

Jatin Tekchandani

Approved:

_____

Chair of the Committee
Yingchun Zhang, Associate Professor,
Department of Biomedical Engineering

Committee Members:

_____

Alexander Tiu, Medical Director,
Department of Sleep Disorders
Kingwood Diagnostic & Rehabilitation Center

_____

Nuri Ince, Associate Professor
Department of Biomedical Engineering

_____

Suresh K. Khator,
Associate Dean,
Cullen College of Engineering

_____

Metin Akay, Professor and Chair,
John S. Dunn Endowed Chair,
Department of Biomedical Engineering

Acknowledgements

I would like to foremost acknowledge my advisor and committee chair, Dr. Yingchun Zhang for his support and guidance. I have developed in many ways over the years we have studied together academically, professionally and personally. It has been an honor to be a part of the team he has led.

I have obtained tremendous value from being a part of the lab and having the opportunity to work with some of the most talented people I have ever met. Thinh Nguyen, Thomas Potter and Nicholas Dias have all been very gracious with their time and knowledge. Their insights and criticisms have helped develop the critical thinking skills required to complete this project.

I also would like to thank my committee member, clinical mentor and medical director, Dr. Alexander Tiu for his support and clinical guidance.

I would also like to thank the lab technician, Alessya Delgado, for her help with the institutional review board process and for obtaining the consent forms with the excellent quality signals for the analysis. The project would not be possible without the data she has so diligently captured.

Thanks to all in the department of Biomedical Engineering over the years for their encouragement and support. I would like to thank all my academic advisors I have had in the department, Dr. Adam Capitano, Dr. Ting Chen, Kaitlin Mallory and Deborah Hernandez.

My sincere gratitude to my family and especially my wife Rachel Qianyunli Tekchandani for always being supportive in all my endeavors. Any accomplishment that I have is only because of her.

USE OF MOTION ARTIFACT FOR THE DETECTION OF RESPIRATORY EFFORT IN POLYSOMNOGRAPHY

An Abstract

of a

Thesis

Presented to

the Faculty of the Department of Biomedical Engineering

University of Houston

In Partial Fulfillment

of the Requirements for the Degree

Master of Science

in Biomedical Engineering

by

Jatin Tekchandani

December 2018

Abstract

Measuring respiratory effort is critical when diagnosing sleep disordered breathing. In this thesis work, the use of detecting respiratory effort by using the movement artifact found in the electromyographic (EMG) and electrocardiographic (ECG) recordings used in polysomnography was investigated. The resulting signals were compared to effort measured with respiratory inductance plethysmography (RIP). The EMG and ECG signals were filtered using the Savitzy-Golay method of smoothing and differentiation of data by simplified least squares to extract the movement artifact. The validity of each resultant waveform was measured using a Pearson product moment correlation coefficient and were studied to determine the most reliable signal. A total of 12 subjects were recorded in a clinical setting, all being evaluated for obstructive sleep apnea. The ability to detect respiratory effort using movement artifact was found to perform best in the masseter. This work shows that movement artifact recovered from the EMG and ECG may be a reliable alternative for the detection of respiratory effort.

Table of Contents

List of Figures

List of Tables

Chapter 1 – **Introduction**

This chapter introduces the background of the disease state that polysomnography (PSG) sets out to diagnose. A review of routine PSG acquisition and analysis is discussed. The chapter concludes with the hypothesis and organization of this thesis.

1.1 Background

Sleep disordered breathing is a condition that affects 40-60% of the population and is defined by episodes of complete or partial airflow cessation[1]. To measure the severity of the condition, a metric called the Apnea-Hypopnea Index (AHI) is used which is quantified by the number of apneas and hypopneas per hour of sleep. The greater the AHI, the greater the severity of the disease and the likelihood of additional complications. The AHI has been shown to correlate to daytime sleepiness, risk of cardiovascular disease and mortality[1].

The classification of a respiratory event can be obstructive, central or mixed. During an obstructive apnea, there is continuation of effort. A central event is classified as a lack of effort while a mixed event begins central and ends obstructive. Various techniques have been used to measure respiratory effort. The current clinical standard is respiratory inductance plethysmography (RIP) which is used widely.[3] Other forms of indirect measurement including Mandibular Movements (MM) and Photo-Plethysmography (PPG) have been proposed.[3]

This research will investigate a potential method of detecting respiratory effort using the motion artifact found in the electromyography (EMG) and electrocardiography (ECG) signals. These sensors are already in place during routine polysomnography to measure muscle and cardiac activity.

The waveform that results from the smoothing of the EMG and ECG signals, which is the known to be a motion artifact, will be cross-correlated to the signal measured with the RIP effort belt. The performance of the resulting waveforms will be compared to the Jawsens, a device used to measure respiratory effort using mandibular movements, in various sleep stages and positions.

1.2 Routine Polysomnography Acquisition

Polysomnography is the gold standard for the diagnosis of sleep disorders including sleep disordered breathing. The standard sensors include electroencephalography (EEG) and electrooculography (EOG) for the determination of sleep stage. Sleep stages are defined as Wake, Non-REM Stage 1, 2, 3 and Stage REM. The submental EMG is also recorded for the detection of bruxism, arousals and REM detection.[2] Airflow is measured using a nasal pressure transducer and a thermistor. These two sensors allow for the detection of reductions and cessations of breathing, called apneas and hypopneas. Respiratory effort is measured routinely with respiratory inductance plethysmography. ECG is also applied for the detection of heart rate and arrhythmias. Blood oxygen saturation is measured using a pulse oximeter which is used for the detection of desaturations. Limb EMG sensors are applied for the detection of abnormal movement disorders in sleep.[2] All of the applied sensors are visualized in Figure 1.1.

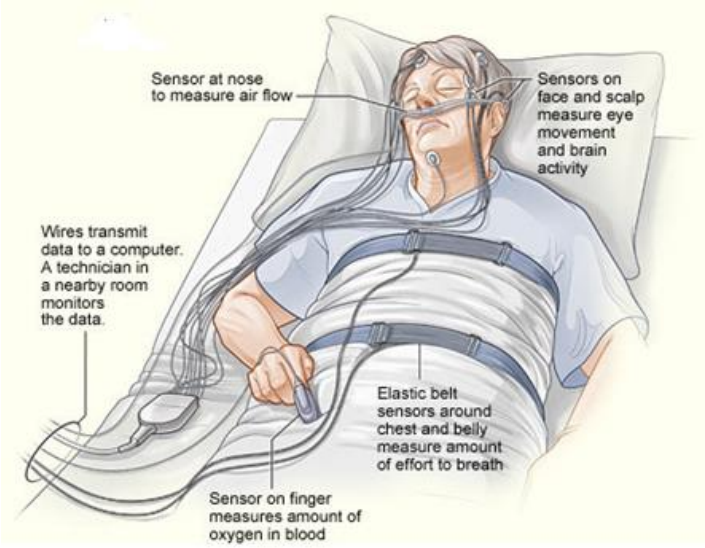

Figure 1.1 Routine Polysomnography demonstrating the ability to detect oximetry, brain and respiratory activity.

1.3 Routine Polysomnographic Analysis

The first step of the acquisition of a polysomnographic record is to identify the sleep stages based on the EEG and EOG data. Figure 1.2 shows the various waveforms from the different sleep stages as seen on the EEG data acquired during routine polysomnography.[1]

As seen in the figure, each stage is defined by the waveforms it contains. Relaxed wakefulness is characterized by alpha waves seen in the occipital electrodes. When the alpha rhythm is replaced with theta waves, the stage transitions to non-REM stage 1. Once spindles and k-complexes appear, the stage is then N2. Delta or slow waves, seen in the frontal derivations, indicate non-REM stage 3. When sawtooth waves are seen in the EEG while chin EMG is reduced, and rapid eye movements are seen in EOG, then the stage becomes Rapid Eye Movement (REM).[2]

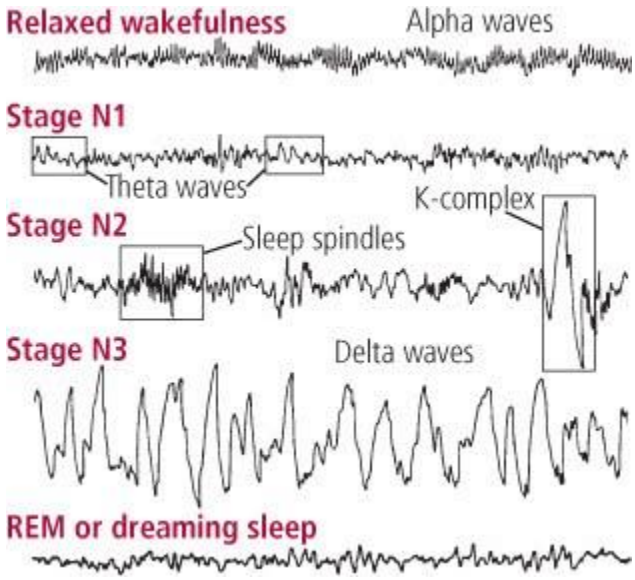

Figure 1.2 The four stages of sleep as seen on the EEG

Once the study has been staged, the analysis of the respiratory signals begins, and all abnormal findings will be measured and tabulated. In figure 1.3, the three types of events are seen. An apnea is defined as an event lasting a minimum of ten seconds with over a 90 percent reduction in airflow. [2] The classification, or type, of the apnea is based on the measurement of respiratory effort. When effort is persistent throughout the event, it is classified as an obstructive apnea. When effort is absent, it is then classified as a central apnea. When effort is absent at the start of the event but then resumes while airflow remains absent, this is called a mixed apnea. When the airflow is reduced but does not meet the criteria for an apnea, the event may be classified as a hypopnea or a Respiratory Effort Related Arousal (RERA). A desaturation associated with the event is required for the detection of a hypopnea. A cortical arousal, measured with the EEG, is required for the detection of a RERA.[2]

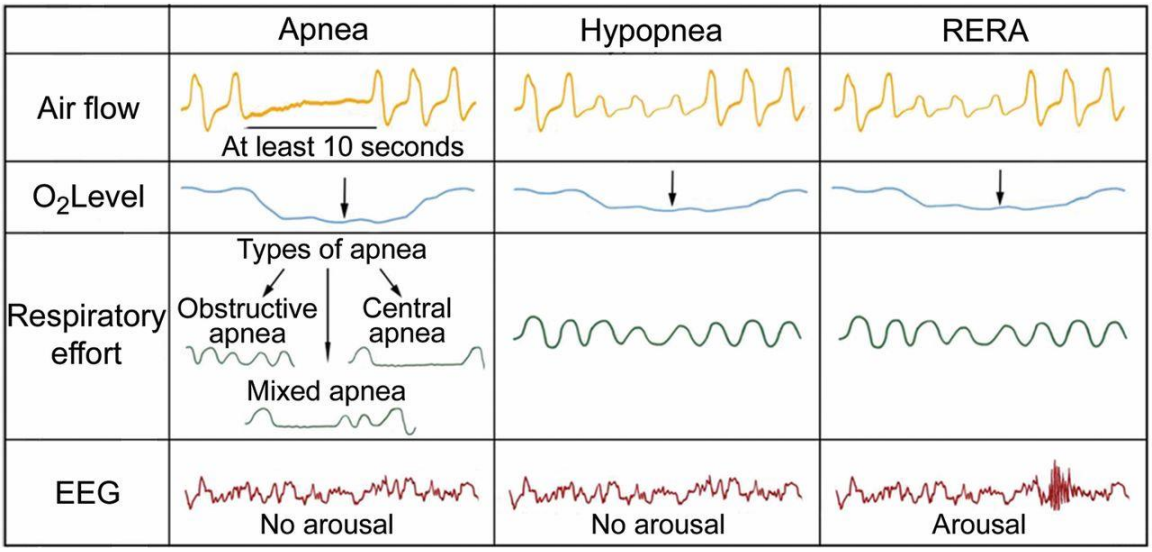

Figure 1.3 Respiratory Event Classification

1.4 Hypothesis and Specific Aim

The thesis will focus on the detection of respiratory effort during polysomnography for diagnosing sleep disordered breathing. The hypothesis of this investigation is that a reliable measure of respiratory effort can be obtained from the use of the motion artifact observed in the EMG and ECG recordings. Four EMG sites, one ECG and the Jawsesns will be compared to determine which has the highest correlation between it and the RIP thoracic effort belt. The hypothesis is that the masseter will outperform all other options.

1.5 Arrangement of Chapters

The thesis continues with chapter two where the methods of how the research was conducted by reviewing the subjects, sensors and processing techniques. The results from the experimental procedure will be covered in chapter three. The discussion of the results and the study limitations will be explained in chapter four. The concluding chapter will summarize the project and offer suggestions for future directions.

Chapter 2 – **Methods**

In this chapter, the subjects recorded will be discussed followed with the sensors used for the measurement of respiratory effort. The signals recorded will be visualized and then imported for analysis into a Python programming environment.

2.1 Subjects

Twelve subjects of both genders were recruited according to a protocol approved by the Institutional Review Board (IRB) of the University of Houston. Each subject was tested for a suspected diagnosis of sleep disordered breathing. All testing was performed at the Kingwood Diagnostic & Rehabilitation Center. Each of the subjects gave written consent to participate in the study. All twelve subjects were found to have obstructive sleep apnea after each recording was scored and interpreted according the guidelines published by the American Academy of Sleep Medicine[2] with details found in Table 2.1. The subjects were those typically referred to the sleep disorders department. The sensors were applied and maintained by a qualified technician with Collaborative Institutional Training Initiative (CITI) certification. Great care was taken to ensure that the research modifications had no impact on the patient's diagnosis.

Table 2.1 Subject Demographics

	Mean	**SD**
Age(y)	58.9	13.2
Sex M/F	8/4	
BMI (kg/m^2)	35.9	6.6
AHI (events/h)	36.1	13.2

2.2 Polysomnography Recording

All the sensors involved in routine polysomnography, as recommended by the AASM[2] were applied for each recording (Philips Respironics Alice, Murrysville, PA USA). The parameters included EEG (F3-M2, F4-M1, C3-M2, C4-M1, O1-M2, O2-M1), right and left EOG, left and right tibialis anterior EMG, thoracic and abdominal RIP, ECG, nasal flow measured with both a pressure transducer and a thermistor, and O_2 saturation by a digital oximeter (Nonin Medical, Plymouth, USA).

In addition to the routine sensors, the Jawsens magnetic distance sensor was applied and included in the recording montage. The EMG of the masseter and temporalis were also included for this investigation.

2.2.1 Hardware specifications

The specifications for the Alice system used for this study are found in Table 2.2 which describe the Sample Size (in bits), which specifies the bit resolution, the recording frequency (in Hertz), for how often the data is recorded per second and the range of values with the units for the channel.

In table 2.3, the specifications for the Brizzy device can be found. The Brizzy is the adapter used to connect the Jawsens to the Alice system for the recording of the mandibular movements. The output of the Brizzy was plugged into the Alice using the Auxiliary input.

Some of the channels are capable of higher recording frequencies that are not routinely used in practice. To ensure that the resultant waveforms could be obtained from a recording using standard settings, the lower option for each channel was used for this study.

Table 2.2 : Alice Hardware Specifications

Channel	Sample Size (bits)	Recorded Frequency (Hz)	Range	Units
EEG	16	200	± 0.30	mV
EOG	16	200	± 0.30	mV
EMG	16	200	± 0.78	mV
ECG	16	200	± 8.33	mV
Airflow	16	200	± 2.64	mV
Effort	16	200	N/A	N/A

The EEG, EOG, EMG, and ECG signals are obtained using AC amplification. The effort and airflow signals are DC. The channels in polysomnography that are AC measure voltage between a single input and a ground. The Brizzy device used to obtain the mandibular movement signal is DC. The RIP module used to measure the thorax is also DC.

Table 2.3 Brizzy Hardware Specifications

Channel	Measurement Range (cm)	Resolution (mm)	Sampling Frequency (Hz)	Units
Mandibular Movement	7-23.5	0.1	10	mV

2.3 Respiratory Inductance Plethysmography

The current clinical standard for the detection of respiratory effort is the RIP sensor. It involves the recording of thoracic and abdominal excursions with sensors sensitive to longitudinal tension.[3] The technique used in RIP is based on the measurement of electrical inductance. The cross-sectional area changes within the bands result in a variation of inductance. This method is currently the preferred method of measuring respiratory effort clinically.[3] An application of a RIP belt sensor to a patient can be seen in figure 2.1.

The belts contain a sinusoid wire coil that is placed into an elastic band. Using frequency demodulation and an oscillator, the digital respiration signal is generated from the measured changes in inductance. Changes in the frequency is converted to a waveform where the amplitude of the waveform is proportional to the inspired breath volume. [3]

Figure 2.1 Respiratory Inductance Plethysmography for the detection of respiratory effort

2.4 Mandibular Movements

It has been found that the measurement of mandibular movements using a magnetic sensor placed midsagittaly could be used to detect respiratory effort.[4] In this study, a device, (Brizzy Nomics, Liege, Belgium) was used to measure the mandibular movements during the polysomnographic recording. The device measures distance in millimeters between the forehead and the chin using two parallel, couples, resonant circuits. One of these circuits is the transmitter and generates pulsed magnetic wave of very low energy at a frequency of 10 Hz. The receiver measures and records the change in the magnetic field and this results in a measure of distance with a resolution of 0.1mm. The application of the Jawsens sensor can be seen in figure 2.2.

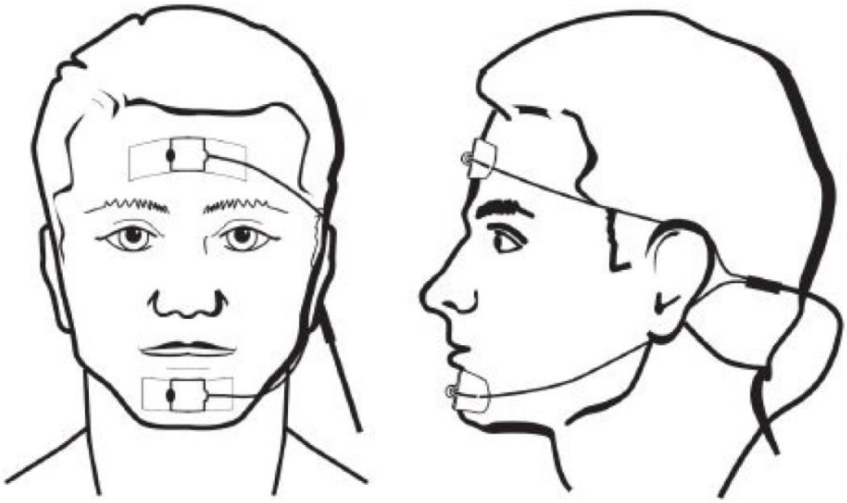

Figure 2.2 The Jawsens sensor with one element taped to the forehead and the other to the chin.

2.5 Masseter and Temporalis Electromyography

The electromyography of the masseter and temporalis muscles are used in the determination of bruxism detection and for the evaluation of temporomandibular joint (TMJ) disorder. The placement of the sensors was based on three lines: TL_V, TL_H and Go.[5]

The TL_V line corresponds to the bony prominence formed by the zygomatic process of the frontal bone and the posterior limit of the front process of the zygomatic bone; the TL_H line corresponds to the upper border of the zygomatic arch. To measure the temporalis, electrodes were placed according the fibers directions of the anterior temporalis muscle, just above the zygomatic arch, posterior to the line TL_V and anterior to the scalp.[5]

To measure the superficial masseter muscle, the line Go was located at the angle of the mandible and body of the zygomatic bone. The Muscle Line (ML) was found from these landmarks and was joined with Go at the midpoint between the lower posterior border of the zygomatic bone and the zygomatic arch. The placement of the electrodes, along with the above-mentioned lines and landmarks can be seen in figure 2.2 and figure 2.3.[5]

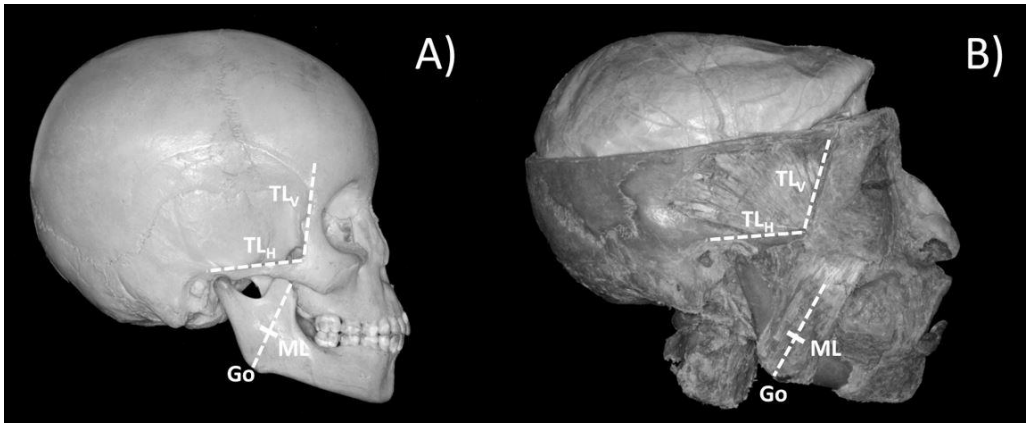

Figure 2.3 A) Lateral view of the skull with reference lines used for the study: TL_V, TL_H, and ML. B) Lateral view of the deep facial planes, evidencing the Anterior temporalis and superficial masseter muscles and their relationship with anatomical landmarks.

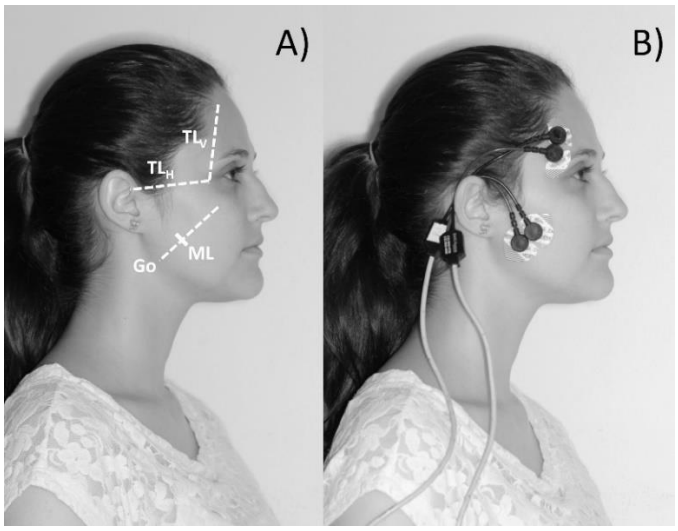

Figure 2.4 A) Reference lines visualized B) Electrode placement

2.6 Polysomnographic Recording

After the application of all the routine and additional sensors, the subjects were recorded using the Alice polysomnography system. Figure 2.5 and 2.6 show the complete

montage including: from the top - the two EOG derivations, six EEG, two jaw EMG, Jawsens, thermistor flow, nasal pressure flow, thoracic RIP, abdominal RIP, snore microphone, two EKGs, heart rate, blood oxygen saturation, photo plethysmography, pulse rate, and two limb EMG leads. Figure 2.5 shows the bio calibration process on a 3-minute window. A visible change can be seen to the Jawsens and Jaw EMG signals when the patient is instructed to yawn. Figure 2.6 is a 30 second time window showing an increased level of detail of the signals.

The signals seen in figure 2.5 and figure 2.6 were filtered for display and scoring according to the recommendations of the American Academy of Sleep Medicine and the values of the filter settings can be seen in table 2.1.

Table 2.4 Filter Settings used for Display and Scoring

	Low Frequency	High Frequency
EEG	0.3 Hz	35 Hz
EOG	0.3 Hz	35 Hz
EMG	10 Hz	100 Hz
ECG	0.3 Hz	70 Hz
Respiratory	.1 Hz	1 Hz

The EMG and ECG signals were not considered respiratory during the display and scoring of the studies. They were only used to detect bruxism activity and to assist in staging. The experimental technique of motion waveform respiration had no impact on the diagnostic results.

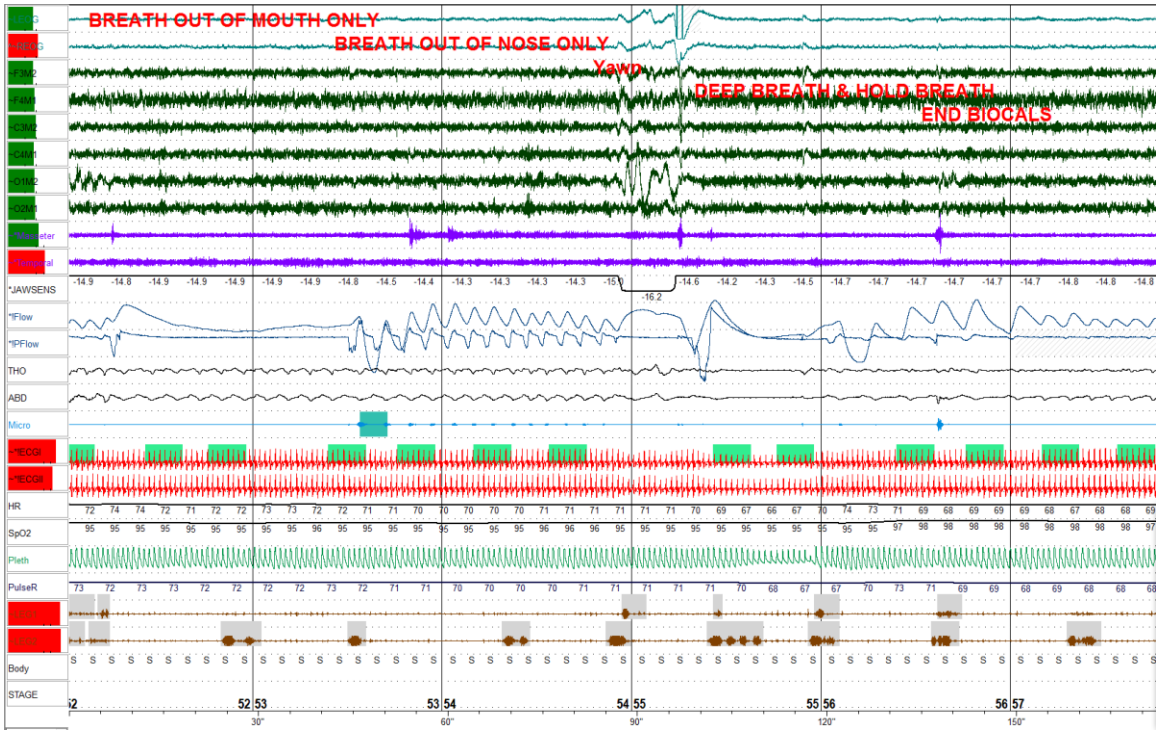

Figure 2.5 Complete montage during bio calibration process in a three-minute window.

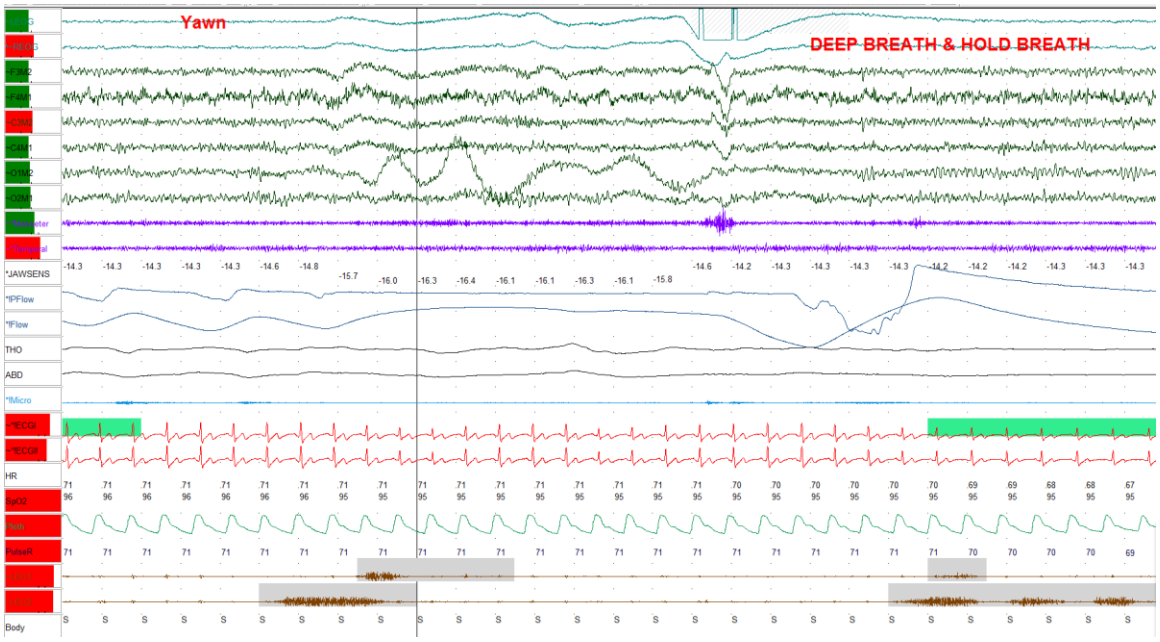

Figure 2.6 A 30 second view of the recording segment of the complete montage.

2.7 Importing the polysomnographic data in Python

Once the recording was complete, all the data was saved to a file using the Alice export to EDF feature. The resulting EDF was then imported into a Jupyter notebook using MNE. [6-7] Using MNE, the EDF was segmented based on epochs and then used to create a data frame object that can be visualized, filtered and analyzed. Figure 2.7 shows a plot of the data frame after being imported into the Python environment with the Jawsens, two EMG sensors, and the two RIP sensors. The Abscissa for all the plots is sample number. All the plots are a measure of voltage as measured from the sensors described previously.

Figure 2.7 is a plot of 30 seconds of raw, unfiltered data after being imported into the Python environment. The 30 second segment is used routinely in polysomnography. Each epoch is staged as either wake, non-REM 1, 2, 3, or REM. The filtered segments are displayed in the next chapter as 10 second segments for improved ability to observe the morphology of the waveforms and compare the differences of the three methods of measuring respiratory effort.

It can be seen clearly in the raw, unfiltered data that the Jawsens can detect respiratory effort as its signal looks very similar to the raw RIP data with a phase reversal. The motion artifact that correlates well with the effort belt can be visualized in the raw data of the ECG. It is not clear from the visualization of the raw data that the EMG signal has a low frequency component that may be related to respiratory effort.

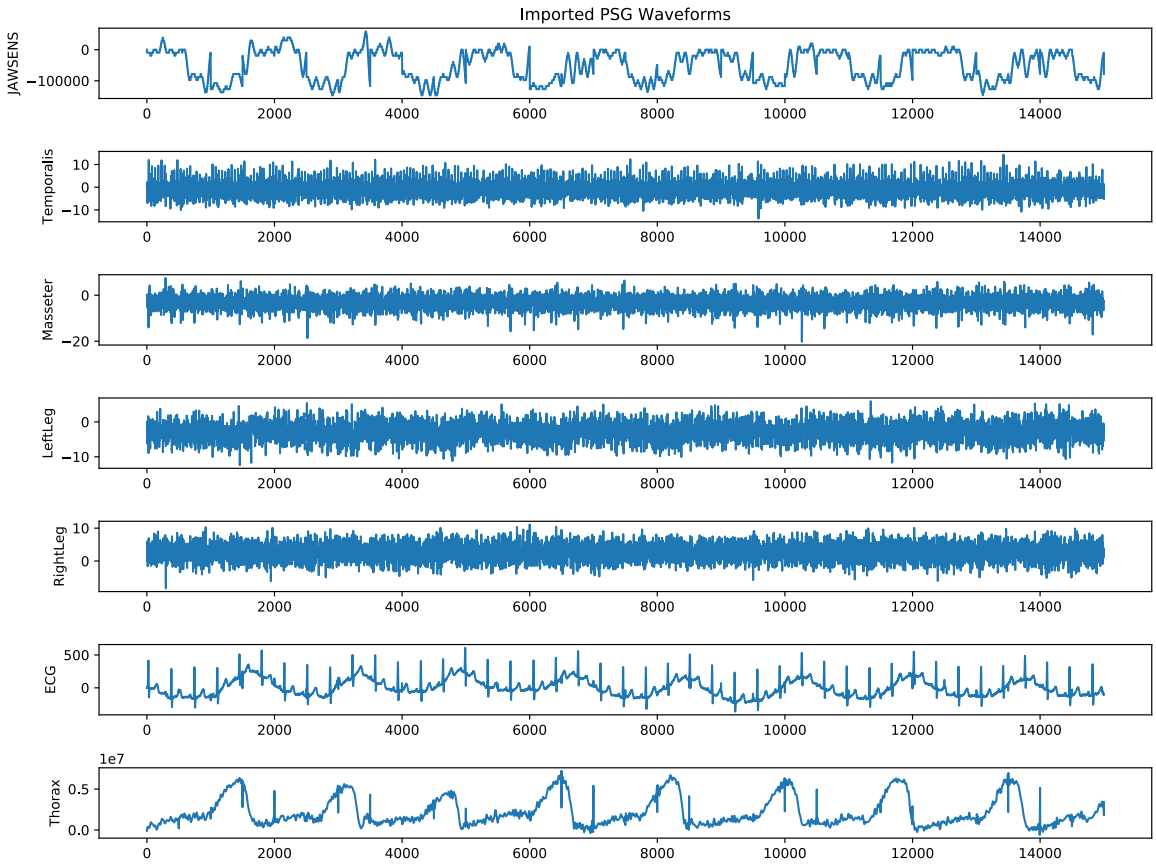

Figure 2.7 A 30 second plot of the raw data after being imported to Python

2.8 Signal Processing

Once the data was successfully imported into Python and each signal into an array, the signal processing can begin. A well-known method of extracting a low frequency component of a signal while maintaining peak levels was found by Savitzy and Golay in 1964 who found that it was possible to smooth data using a polynomial approximation that is based on local least squares.[7-8] Applying the Savitzy-Golay filter to

the signals shown above resulted in what can be seen in figure 2.8 where the processed EMG and ECG have a visual similarity with to the effort sensors.

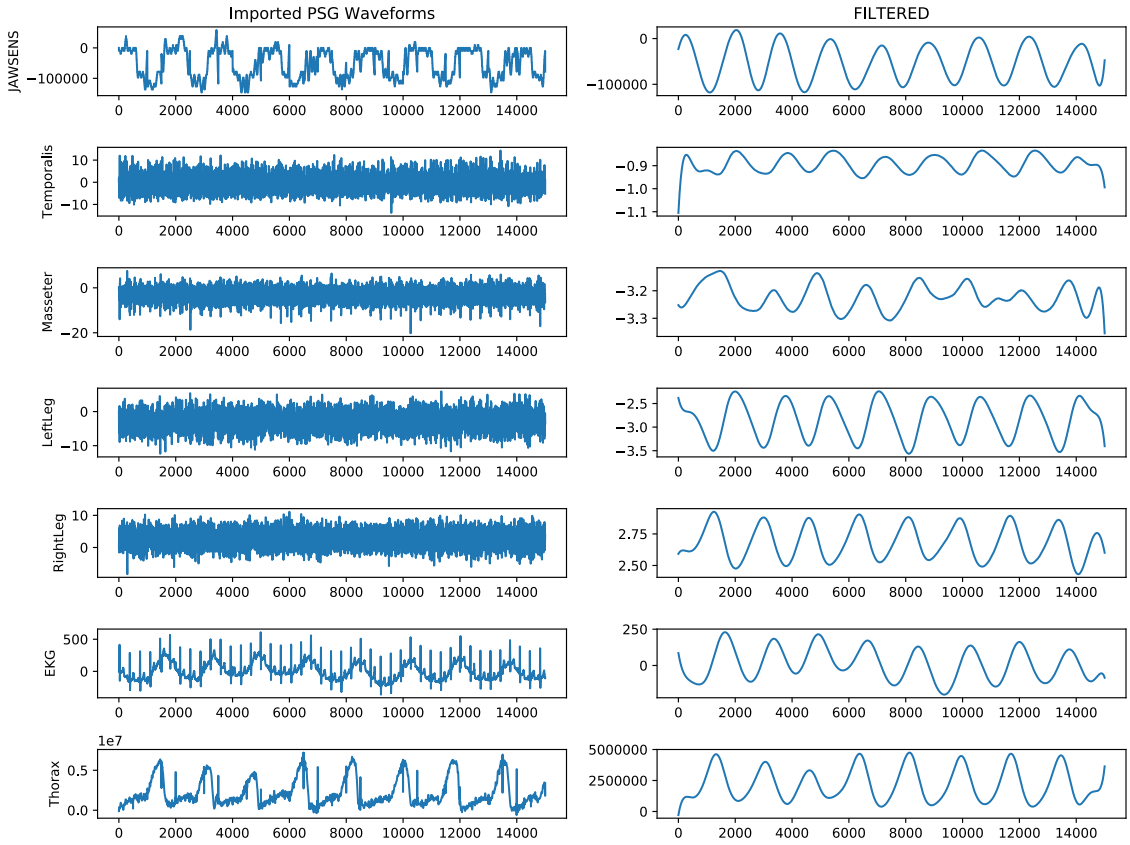

Figure 2.8 30 second plots of data before and after filter has been applied

The filter was applied using a window size of 1711 samples with a polynomial order of 5. The parameters used for the filter determine its frequency characteristics. The values chosen to allow for respiratory effort to be extracted while maintaining some of the higher frequencies that may be needed for the detection of abnormal respirations. This filtering process was applied five times for increased smoothing. The same filtration process was applied to all the waveforms before the Pearson product-moment correlation coefficients were tabulated.

Chapter 3 **Results**

This chapter will review the measurements of the seven sensors and demonstrate their clinical usefulness by displaying the resulting filtered plot next to the raw unfiltered data. One plotted ten second segment from each subject will be displayed and briefly discussed. The calculations of the cross-correlation coefficients will be tabulated for each segment. The effectiveness of the signal is seen as its ability to reproduce what is detected by the RIP sensor visually as well as measured using the cross-correlation coefficient.

3.1 Subject 1

The first recording in this study was able to demonstrate that filtering the EMG signal results in a signal that correlates well with respiratory effort. This was validated by the similarity of the result to the raw signal of the RIP sensor. In Figure 3.1, a ten second segment of data is plotted where the filtered EMG signal very closely matched the output of the RIP sensor.

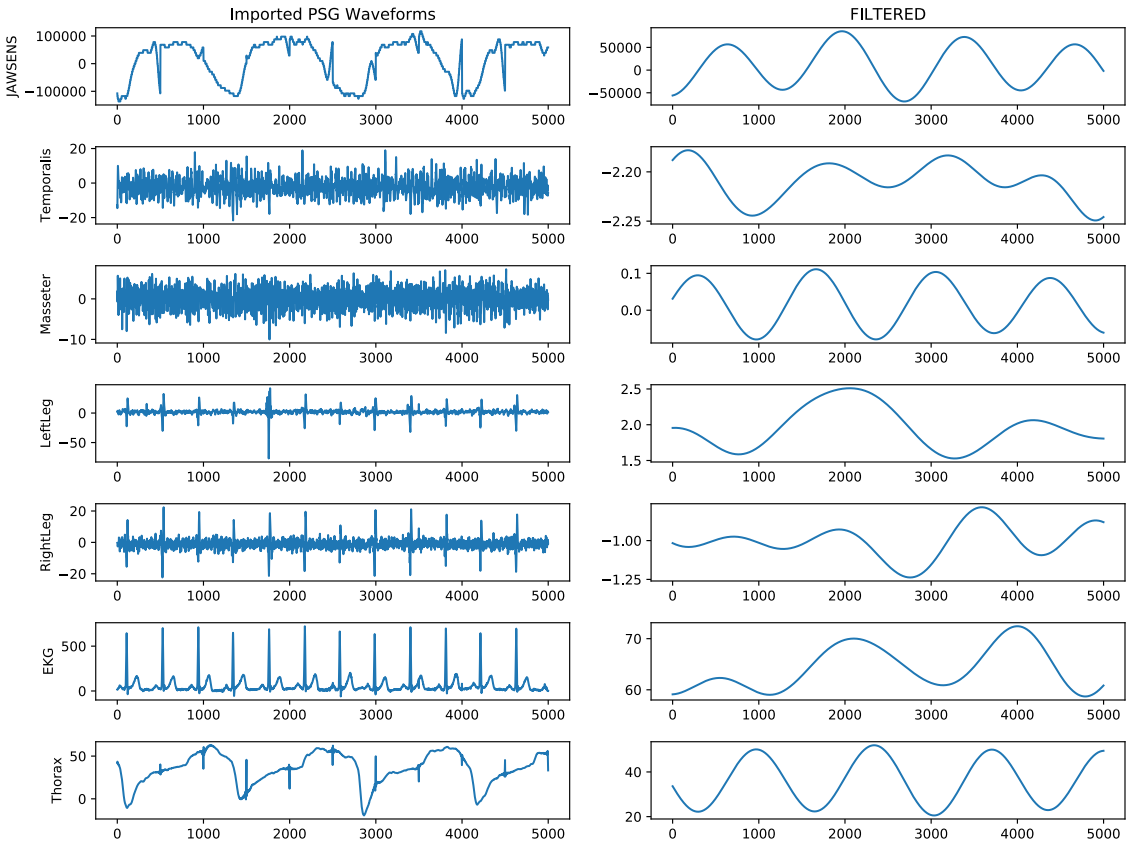

Figure 3.1 Plots from a ten second segment of data from Subject 1's recording.

The cross-correlation coefficients for this ten second segment can be seen in Table 3.1. This value is the focus of this project as it is the measure of how well the motion artifact waveform method performs. In this segment, the value is negative of the Masseter as the signals are out of phase. This does not reduce the effectiveness or clinical significance of the signal and is very easily correctable. The value of -0.98 indicates that the two signals are nearly identical, except for the phase difference.

The phase difference is dependent on how the acquisition was setup, and how each channel was plugged in. For the AC channels, such as the EMG and ECG, one channel is subtracted from the other, with one of the inputs being 1 and the other 2. The decision for which electrode is 1 causes the polarity reversal. These decisions are made at the time of

acquisition and are different for each subject. The phase difference is correctable either in hardware or software. When visualizing the waveforms, the ability to invert the tracing is available. There is also the option of reversing the polarity of the inputs during the setup of the acquisition. The smoothed signal was not available to the technician during the hookup and so it could not have been corrected at that time.

The cross-correlation coefficient measurement is a measure of similarity between each waveform and the one obtained from the RIP belt. It is calculated for each ten second segment. The segments will be grouped by stage and position with their results tabulated and plotted in the Analysis section of this chapter. In this section of the chapter, one segment with their waveforms is displayed with their correlation values as an example of the data that is studied in the analysis section.

Table 3.1 RIP Cross Correlation Coefficients from Subject 1 Data Segment

Jaw	Masseter	Temporalis	Left Leg	Right Leg	ECG	Stage
0.1968	-0.9916	-0.6812	-0.04112	0.4074	-0.1603	N2

3.2 Subject 2

The next ten second segment that will be discussed originates from the second recording of the study. In Figure 3.2, the three signals are shown in their raw state on the left and then after signal processing on the right. In this segment, all the filtered signals correlate well with the RIP belt except for the Jawsens and Temporalis. A waveform recovered from a motion artifact may be able to out-perform a device intended to measure respiratory effort.

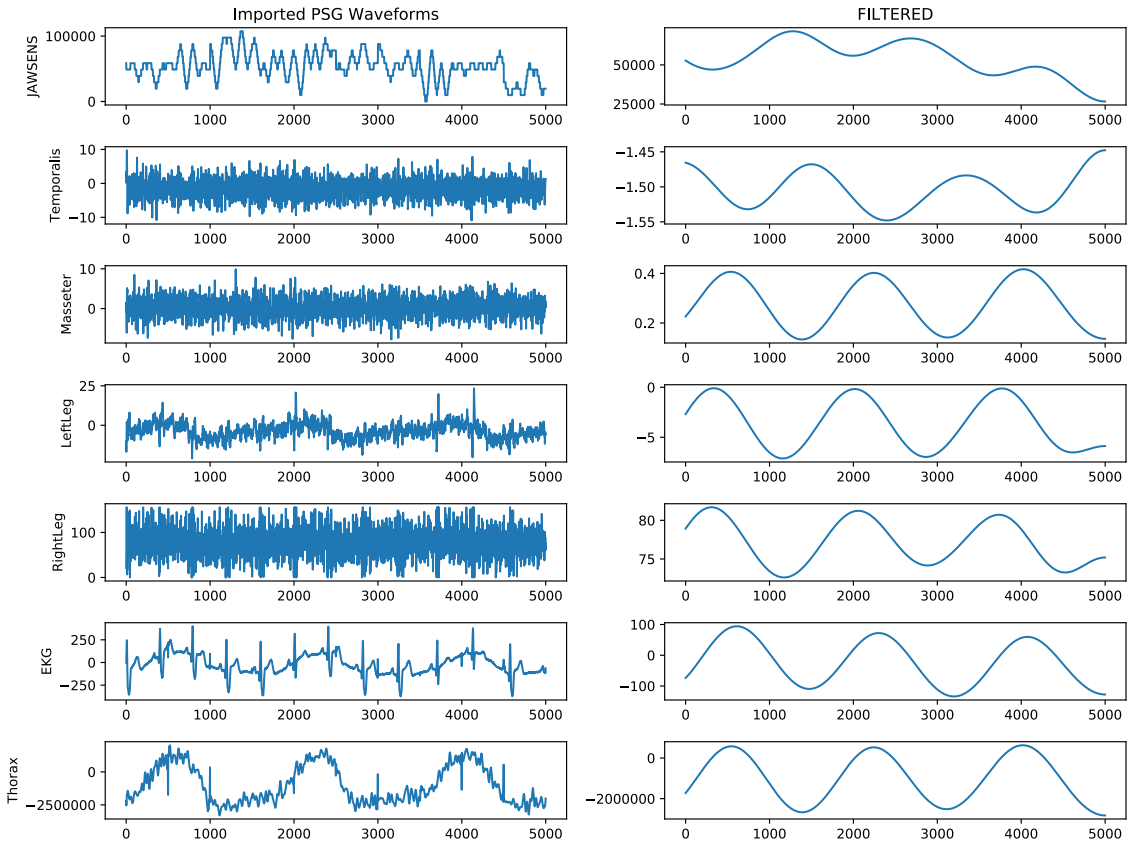

Figure 3.2 Plots from a ten second segment of data from Subject 2's recording.

In this ten second segment, some of the filtered signals produce a waveform that is visually nearly identical to the filtered RIP waveform and very also like the plot of the raw RIP. With this segment, the credibility of the motion artifact method becomes clear. In Table 3.2 the cross coefficients of this segment are tabulated. The Masseter coefficient in this segment was the highest with the ECG a very close second with both in the correct phase.

Table 3.2 RIP Cross Correlation Coefficients from Subject 2 Data Segment

Jaw	Masseter	Temporalis	Left Leg	Right Leg	ECG	Stage
-0.0739	0.9986	-0.4836	0.6577	0.5974	0.9479	N1

3.3 Subject 3

This pattern continues with the next recording, where the plots can be seen in Figure 3.3. This ten second segment is very significant as it demonstrated the ability of the filtered waveforms to not only measure respiratory effort, but also the lack of effort. The ability to classify central and mixed apneas requires a period with reduced or absent effort. This ability is seen in this segment. This segment also shows another example where the phase is reversed between the two methods in some channels. Another observation in the raw data of all the sensors is the simultaneous increase in amplitude when effort resumes.

This is also the first segment where the Jawsens performed well at detecting the effort. The segment shows two breaths where the first is reduced to a level considered absent. Some of the filtered EMG waveforms did not appear to detect this reduced breath. This could be due to the physiological reason where the breath wasn't strong enough to make a change measurable with motion artifact or may have been a consequence of the filtering method. It is likely not the filtering technique, as it did not influence the RIP signal.

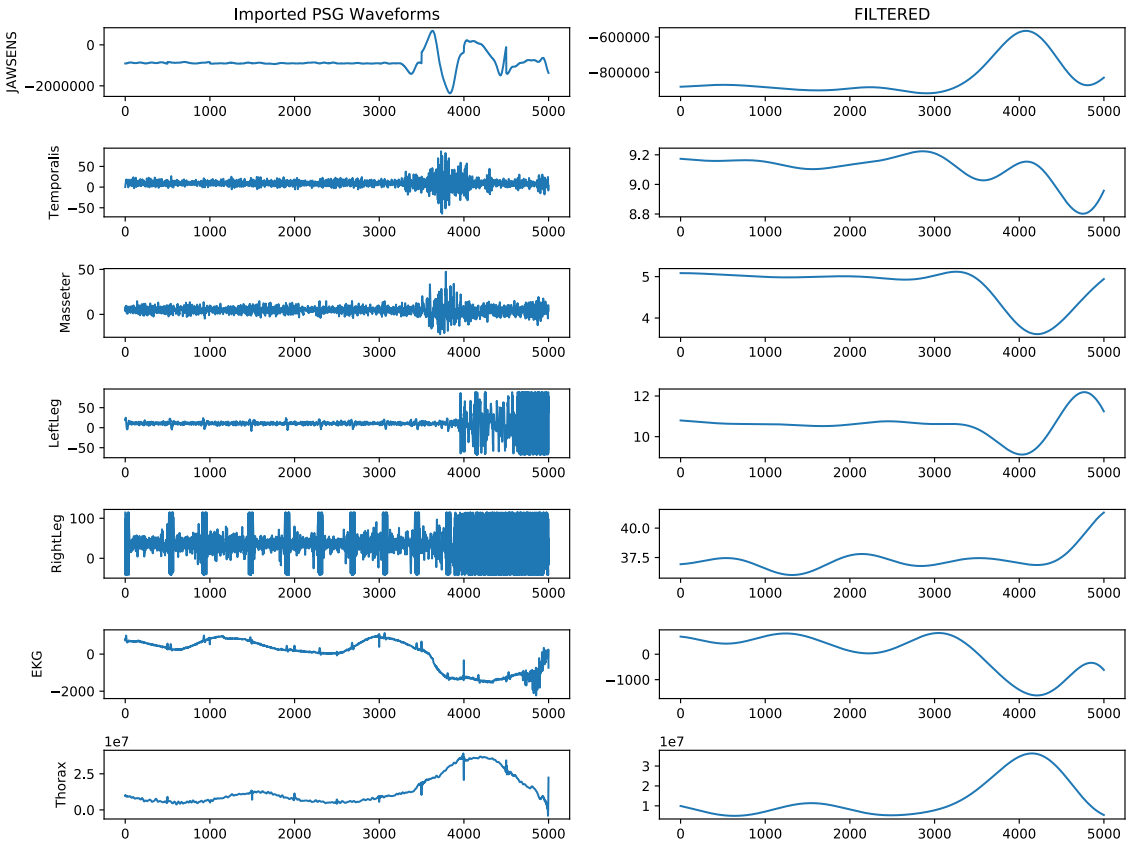

Figure 3.3 Plots from a ten second segment of data from Subject 3's recording.

This segment also demonstrates a high negative cross correlation of the RIP-EMG. In this example, the Jawsens also correlated well with the RIP data. The absolute correlation coefficient was higher than any of the examples seen so far.

Table 3.3 RIP Cross Correlation Coefficients from Subject 3 Data Segment

Jaw	Masseter	Temporalis	Left Leg	Right Leg	ECG	Stage
0.9424	-0.9345	-0.2405	-0.4896	0.1914	-0.8556	N2

3.4 Subject 4

In this plot, we can see a ten second segment of data from Subject 4. In this segment, it is most interesting to note that the third breath was seen to have a higher amplitude observed in the raw RIP signal and in some of the movement artifact waveforms.

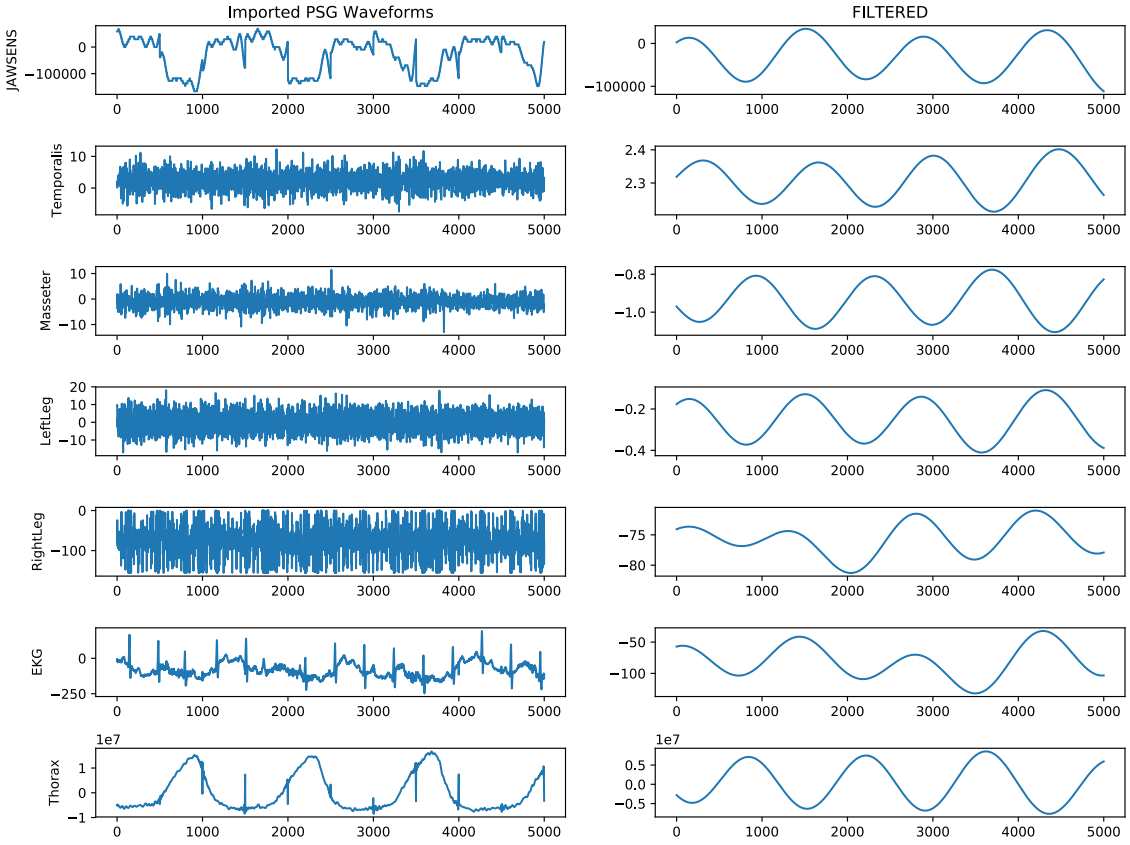

Figure 3.4 Plots from a ten second segment of data from Subject 4's recording.

The cross-correlation coefficients calculated from the above segment can be seen in Table 3.4. In this example, the Jawsens produced a cross correlation coefficient that was the largest in magnitude but was out of phase. The Masseter was second for this segment. All the filtered channels did produce a visible slow wave that did correlate well with the respiratory effort. The performance of the limb EMG is unexpectedly high.

Table 3.4 Cross Correlation Coefficients from Subject 4 Data Segment

Jaw	Masseter	Temporalis	Left Leg	Right Leg	ECG	Stage
-0.9767	0.9185	-0.8560	-0.9491	-0.6899	-0.8344	N2

It will be seen in the Results section of the results how each sensor was able to correlate with the belt for each stage and position. It is in that section that the performance will be measured.

3.5 Subject 5

The plot visualized in figure 3.5 is from a ten second segment of data from subject 5. In this segment, both the filtered Jawsens and the EMG resemble the raw RIP signal.

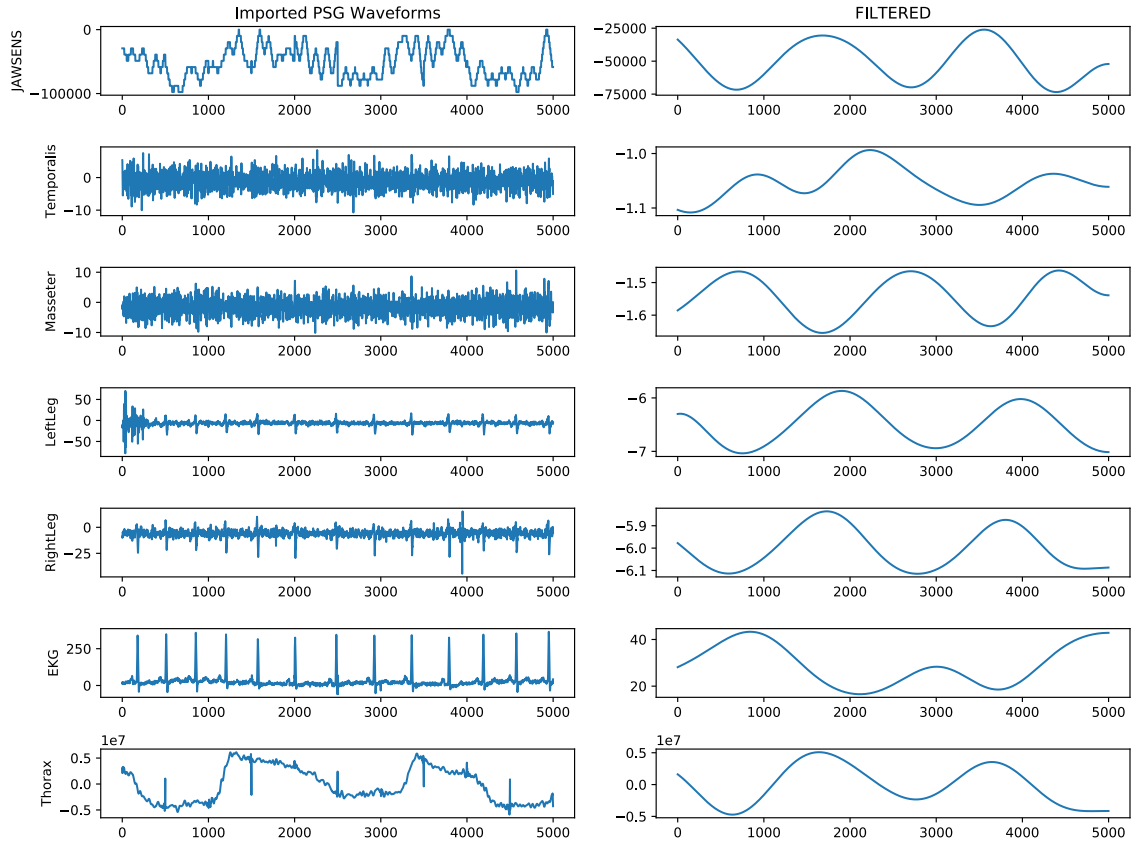

Figure 3.5 Plots from a ten second segment of data from Subject 5's recording.

The cross-correlation coefficients from this segment report that two of the EMG sensors were able to outperforms the Jawsens in a measure of absolute value of the cross-correlation coefficient.

Table 3.5 Cross Correlation Coefficients from Subject 5 Data Segment

Jaw	Masseter	Temporalis	Left Leg	Right Leg	ECG	Stage
0.8880	-0.9247	-0.11206	0.7244	0.9259	-0.7256	N3

3.6 Subject 6

A ten second segment of data from the recording of Subject 6 is seen in Figure 3.6. This segment contains an example of a ECG artifact in the EMG. This example shows how the filtering method performs in a difficult state like that seen in the recording of Subject 6.

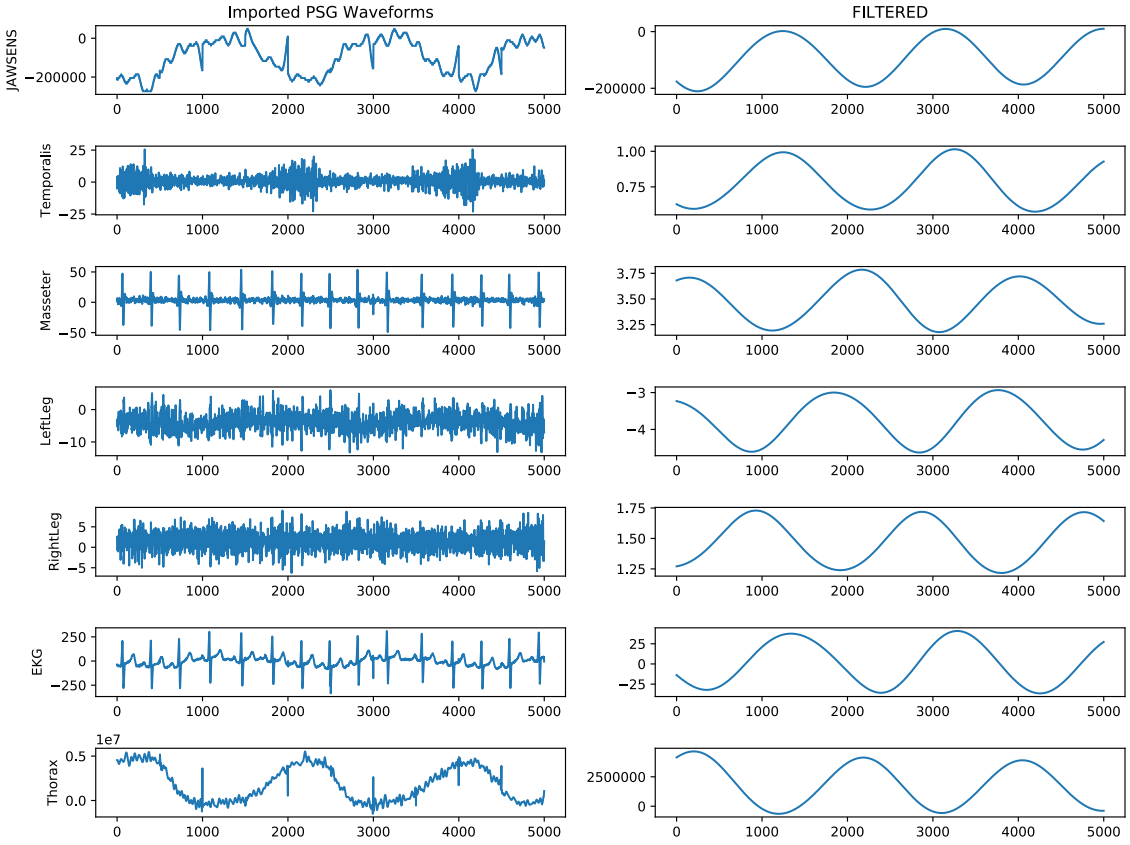

Figure 3.6 Plots from a ten second segment of data from Subject 6's recording.

Despite the noisy signal found in the EMG, the cross-correlation coefficient measured after the filter has been applied shows a strong performance for the method. The highest absolute value comes from the cross correlation between the Jawsens and the RIP. Also observed is that the Jawsens is now out-of-phase while the EMG is in-phase.

Table 3.6 Cross Correlation Coefficients from Subject 6 Data Segment

Jaw	Masseter	Temporalis	Left Leg	Right Leg	ECG	Stage
-0.9949	0.9643	-0.9093	0.5864	-0.6892	-0.8253	N2

3.7 Subject 7

The plot of a ten second segment of data from Subject 7 is seen in figure 3.7. In this segment, the edges on both sides of the segment are distorted and do not represent the raw data well. This is due to windowing method used by the filtering method. At the start of the segment, there is no access to the previous segment. A different windowing method may be able to resolve this type of artifact.

This artifact is one of the reasons why the same filtering method was applied to all the signals before display and cross correlation has been calculated. The artifact effect is equal to all the signals and so the coefficient is still a valid measure of similarity.

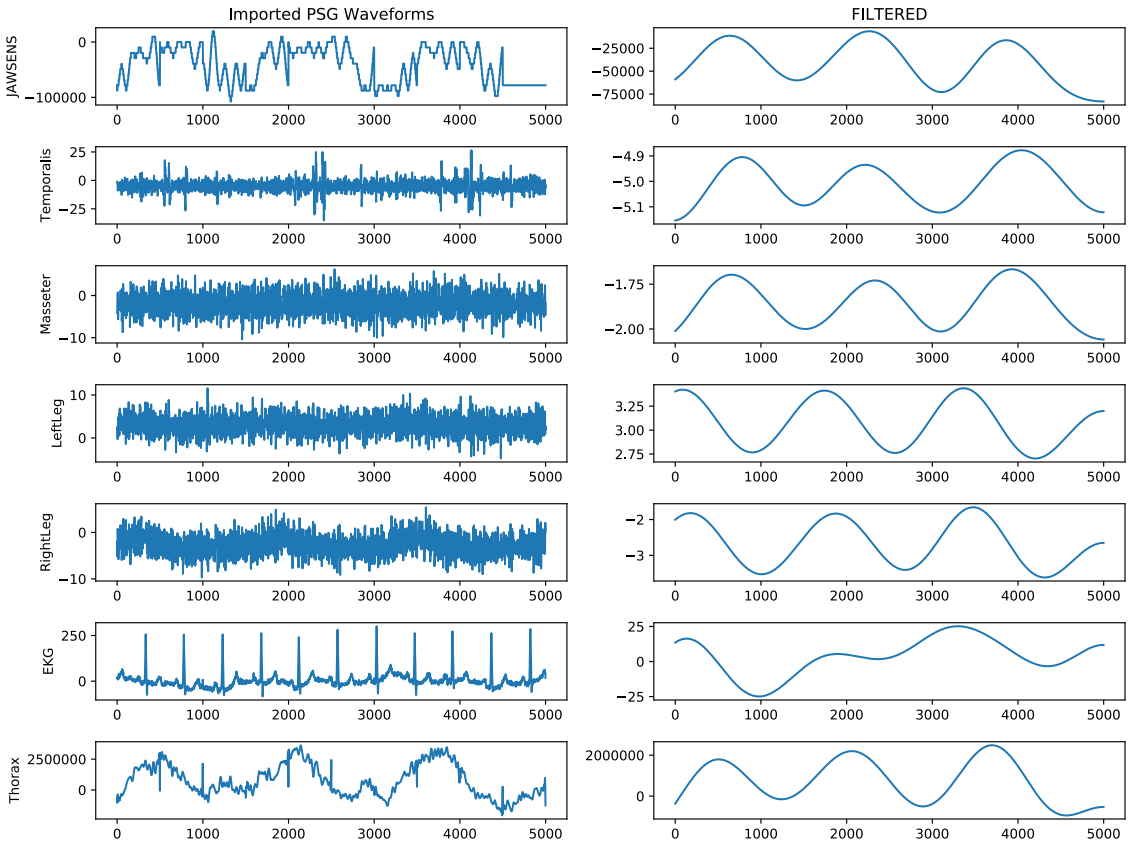

Figure 3.7 Plots from a ten second segment of data from Subject 7's recording.

The cross-correlation coefficients from the subject 7 segment can be seen in Table 3.7. The coefficients are not very high compared to some of the previously seen segments. However, the filtered signals do have a strong visual resemblance to the raw RIP data and so many of the lower cross correlated readings still are able to detect effort on a level that can be clinically useful.

Table 3.7 Cross Correlation Coefficients from Subject 7 Data Segment

Jaw	Masseter	Temporalis	Left Leg	Right Leg	ECG	Stage
0.7702	0.5880	0.4536	0.3101	0.6327	0.1832	N2

3.8 Subject 8

In the ten second segment from subject 8, a slower respiratory rate is observed than has been observed in the previous segments and this is visualized in figure 3.8.

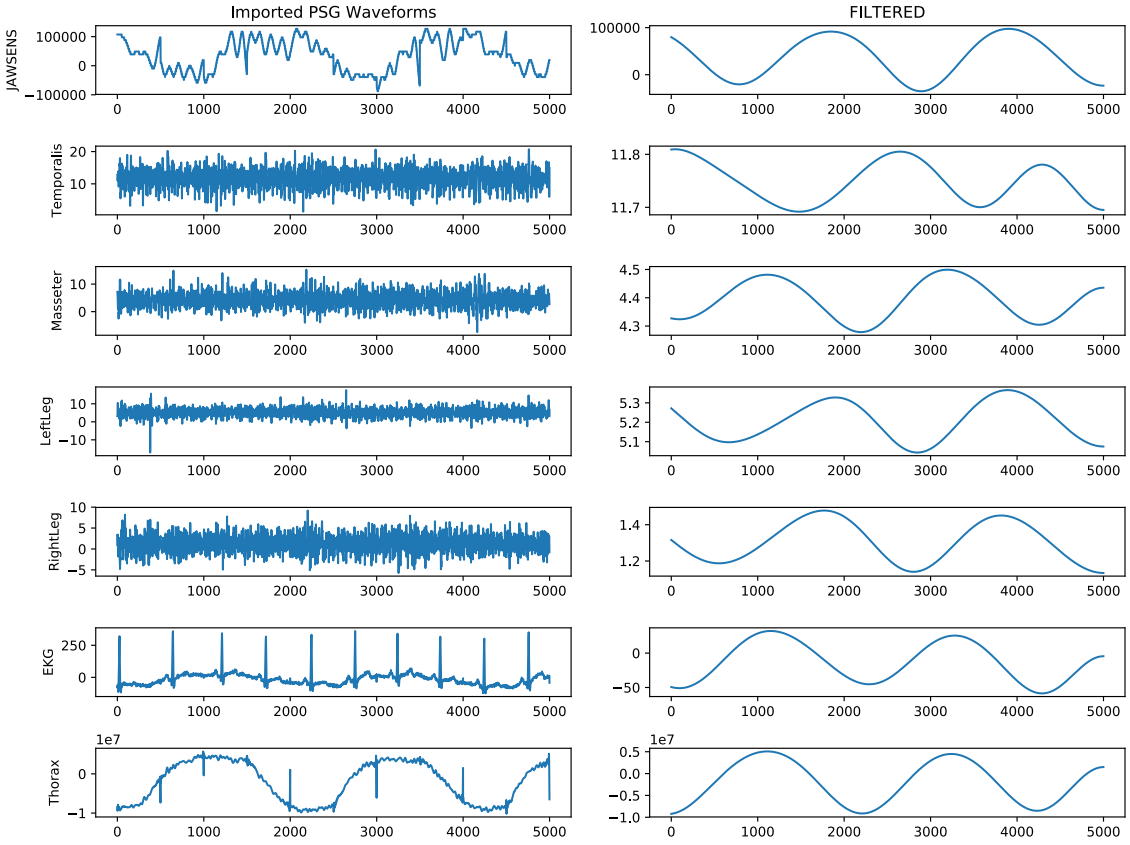

Figure 3.8 Plots from a ten second segment of data from Subject 8's recording.

In this segment, the RIP-EMG cross correlation of 0.98 was not only very high but also in phase. The ECG also had a very high correlation value in the segment of data.

Table 3.8 Cross Correlation Coefficients from Subject 8 Data Segment

Jaw	Masseter	Temporalis	Left Leg	Right Leg	ECG	Stage
-0.5278	0.9871	-0.5799	-0.4550	-0.1732	0.9664	N2

3.9 Subject 9

In Figure 3.9, plots from Subject 9 are seen. In this ten second segment, the low frequency component that correlates with the respiratory effort signal can be seen in the raw data. This is another example where the phase has been reversed. It also observed that the Jawsens did not perform as well in this segment compared to the previous sets of samples.

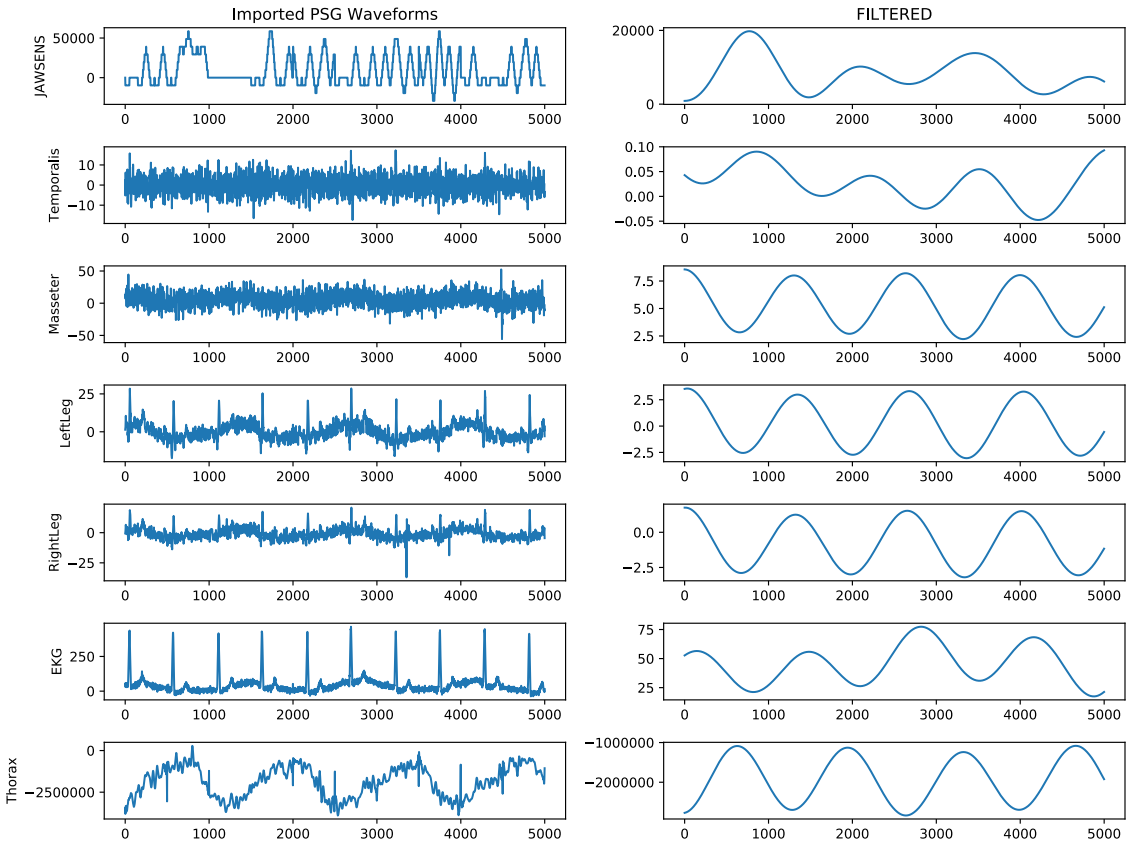

Figure 3.9 Plots from a ten second segment of data from Subject 9's recording.

The results from the cross-correlation calculations for the above figure can be seen in Table 3.9. A very high absolute value was observed with the RIP and Masseter while the Jawsens did not perform as well. All the signals were in the same phase in this segment.

Table 3.9 Cross Correlation Coefficients from Subject 9 Data Segment

Jaw	Masseter	Temporalis	Left Leg	Right Leg	ECG	Stage
0.5165	-0.9630	0.3609	-0.9309	-0.9516	-0.7090	N1

3.10 Subject 10

Figure 3.10 contains the plots obtained from a ten second segment of data on Subject 10's recording.

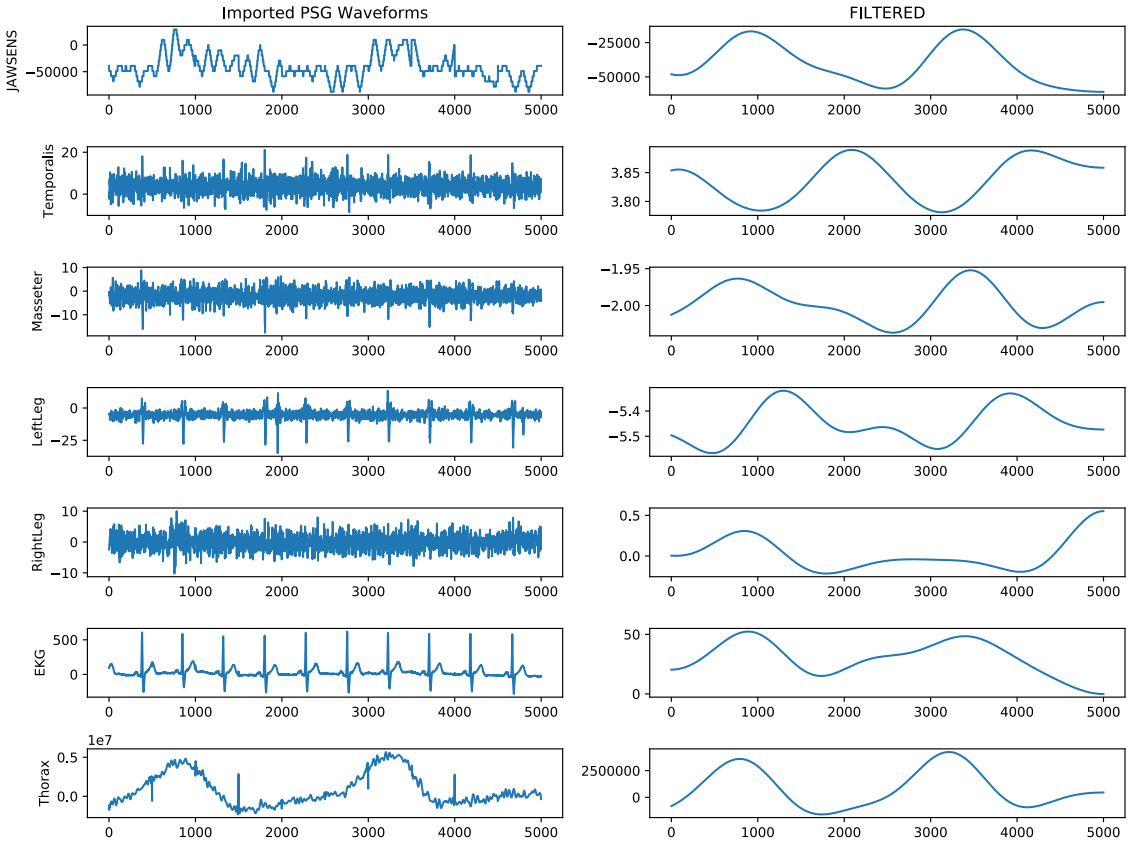

Figure 3.10 Plots from a ten second segment of data from Subject 10's recording.

The cross-correlation coefficients from subject 10's segment above are seen in table 3.10. All the plots in this segment are in phase and the highest cross correlation is the

Jawsens. All the filtered signals do look very similar visually and the filtered EMGs result in a signal that has a morphology like that seen in the Jawsens.

Table 3.10 Cross Correlation Coefficients from Subject 10 Data Segment

Jaw	Masseter	Temporalis	Left Leg	Right Leg	ECG	Stage
0.7365	0.6806	-0.8375	-0.3713	0.3930	0.7489	N3

3.11 Subject 11

The plots from a ten second segment from subject 11 are seen in Figure 3.11.

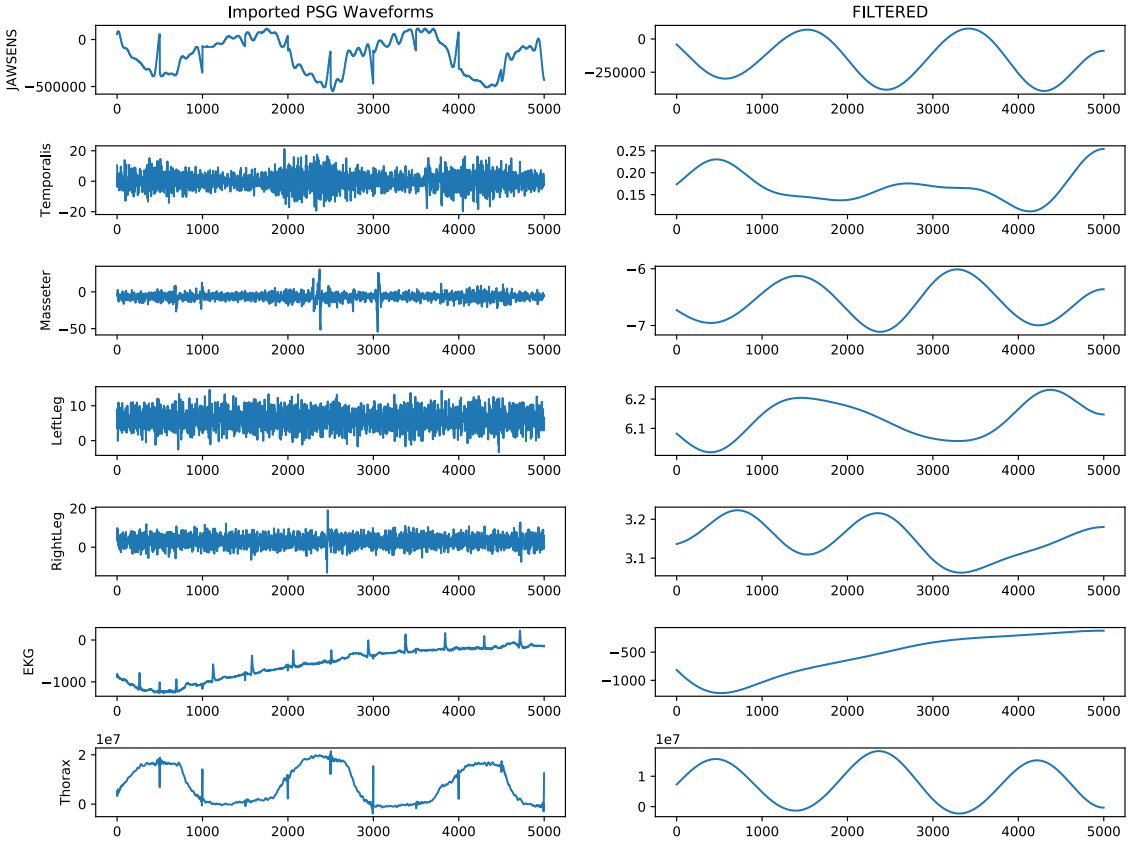

Figure 3.11 Plots from a ten second segment of data from Subject 11's recording.

The cross-correlation results from Subject 11 are seen in Table 3.11. The middle breath, as seen in the raw RIP data does appear to have a greater amplitude when compared to the neighboring breaths. It is observed that in the filtered masseter, this quality of the signal was maintained. The cross-correlation coefficient for the RIP and masseter is very high and is out of phase.

Table 3.11 Cross Correlation Coefficients from Subject 11 Data Segment

Jaw	Masseter	Temporalis	Left Leg	Right Leg	ECG	Stage
-0.8982	-0.9817	0.0998	-0.0180	0.6725	-0.1673	N2

3.12 Subject 12

The final subject for this study, number 12, has the data from a ten second segment plotted in Figure 3.12 below.

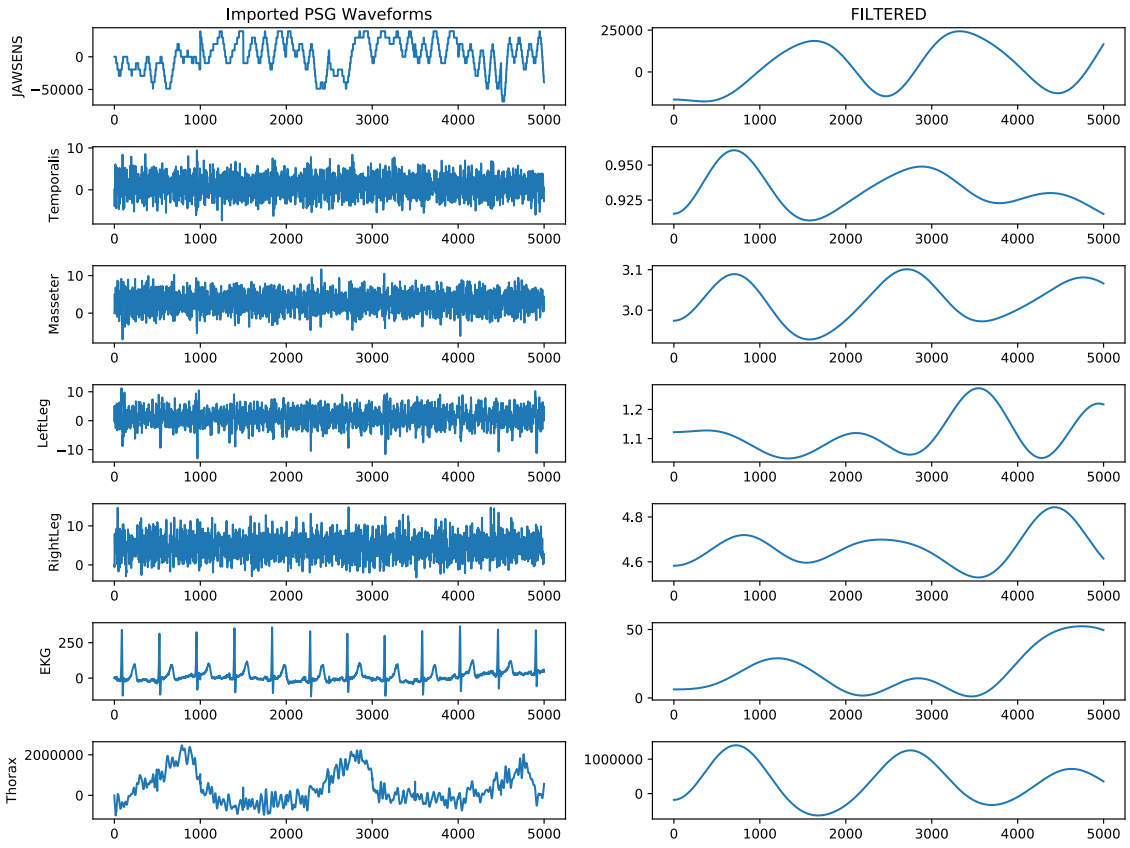

Figure 3.12 Plots from a ten second segment of data from Subject 12's recording.

Tabulated below in Table 3.12 are the coefficients from the cross-correlation calculations. The waveform that resulted from the smoothing of the ECG signal did not have a high correlation in this segment. There did not appear to be enough of a low frequency component in the original signal to recover for the determination of respiratory effort.

Table 3.12 Cross Correlation Coefficients from Subject 12 Data Segment

Jaw	Masseter	Temporalis	Left Leg	Right Leg	ECG	Stage
-0.5429	0.9563	0.8281	-0.0961	0.4688	0.1874	N2

3.13 Analysis

All the cross correlations from the twelve subjects have been combined into a single dataset. All segments that did were labeled as awake or disconnected were discarded. The ability to measure effort while awake using the methods of Jaw distance or motion artifact are not possible when there is voluntary activity and movement such as talking, chewing, or other movements. Also, while awake, the belts were subject to non-respiratory motion that also resulted in the impairment of the ability to detect respiratory effort. Each sleep segment was further divided into Stage 1, 2, 3 and REM. The position of the subject was classified as left, right and supine. The absolute value of the cross correlations of all twelve subjects were then plotted as seen below. The descriptive statistics were also tabulated.

3.13.1 Stage 1

A boxplot of all the cross-correlation coefficients from ten second segments classified as Stage non-REM Stage 1 is seen in figure 3.13. Each column of the boxplot represents that sensor's ability to cross correlate with the RIP belt. RIP-JAW is the measurement of between the RIP sensor and the Jawsens. RIP-MAS is the RIP and Masseter muscle, RIP-TEM is the RIP and Temporalis muscle, RIP-LLG is the RIP and the Left Tibialis Anterior muscle, RIP-RLG is the Right Tibialis Anterior, RIP-EKG is the RIP and the ECG. The Masseter has the highest correlation in terms of the median and mean while in the stage 1 condition.

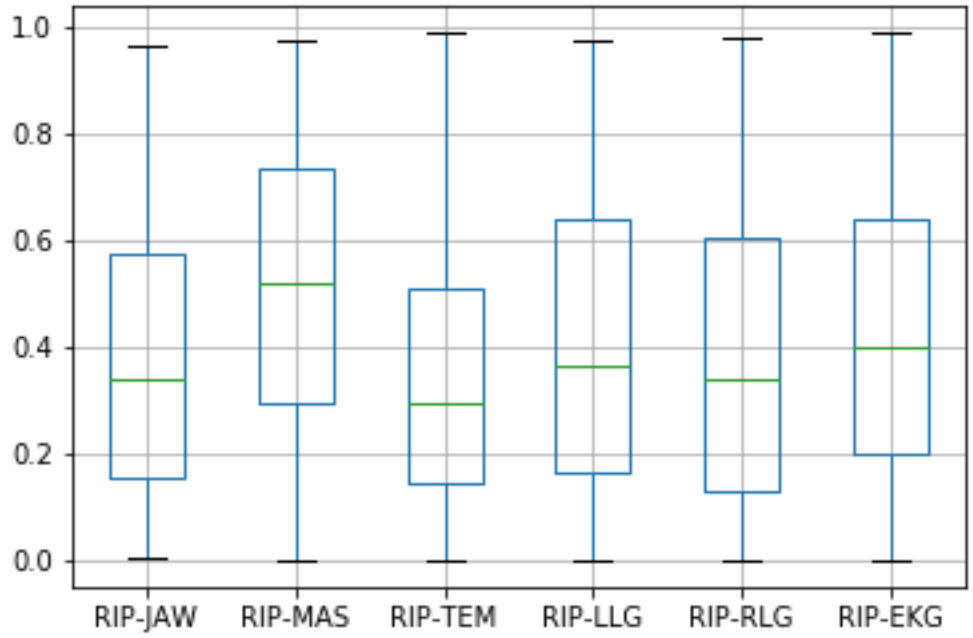

Figure 3.13 Boxplot of Stage 1 segments cross correlation coefficients

The descriptive statistics from stage 1 segments are seen in table 3.13.

Table 3.13 Descriptive Statistics for the cross-correlation coefficients for stage 1

	Jawsens	Masseter	Temporalis	Left Leg	Right Leg	ECG
count	584	584	584	584	584	584
mean	0.406864	0.565148	0.425485	0.443051	0.418736	0.447753
std	0.268725	0.279182	0.258267	0.282520	0.281521	0.271570
min	0.001115	0.002126	0.000477	0.000132	0.001084	0.000942
25%	0.182887	0.323727	0.208881	0.186914	0.157253	0.214794
50%	0.369168	0.600218	0.394293	0.407611	0.416478	0.426605
75%	0.616261	0.816762	0.640864	0.668479	0.660996	0.667905
max	0.992166	0.986471	0.991370	0.984228	0.988219	0.991524

3.13.2 Stage 2

A boxplot of the cross-correlation coefficient calculations for all the segments that were classified as Stage 2 can be seen in Figure 3.14.

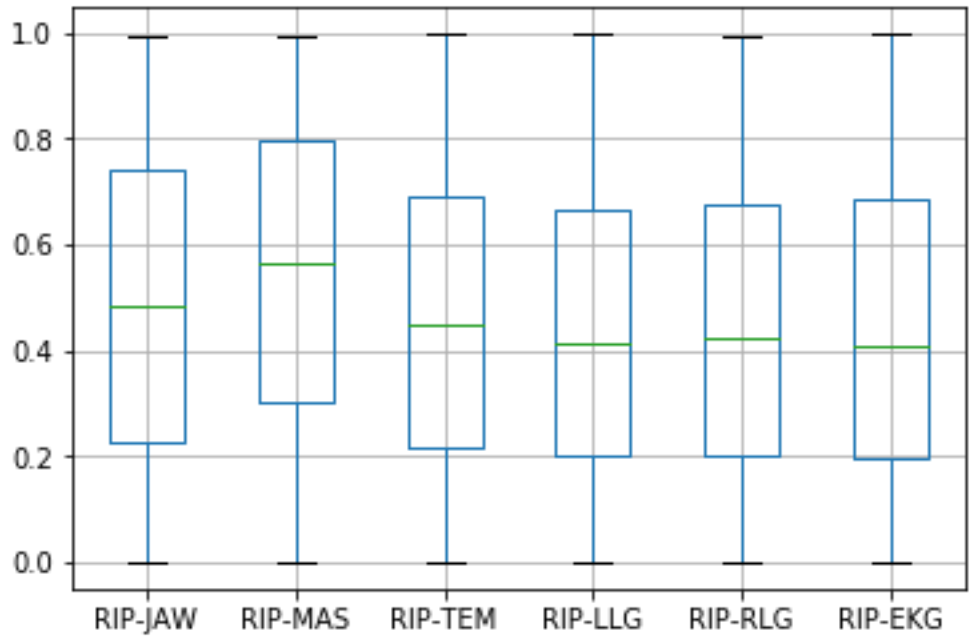

Figure 3.14 Boxplot of Stage 2 segments cross correlation coefficients

A table describing the above boxplot can be seen in Table 3.14. Most of all sleep segments were classified as stage 2 and so the count was higher for this stage than any other. In stage 2, the highest magnitude average and median cross correlation was achieved using the Masseter. The Jawsens was very close in this stage of sleep.

	Jawsens	Masseter	Temporalis	Left Leg	Right Leg	ECG
count	14620	146200	14620	14620	14620	14620
mean	0.484766	0.542227	0.459520	0.441845	0.446432	0.443202
std	0.288770	0.285889	0.276415	0.279652	0.281326	0.285537
min	0.000057	0.000046	0.000052	0.000020	0.731283	0.000032
25%	0.228090	0.301828	0.219001	0.202628	0.201756	0.194016
50%	0.483788	0.567135	0.449449	0.414043	0.421819	0.410206
75%	0.739217	0.796227	0.692511	0.666609	0.677661	0.684697
max	0.995876	0.996116	0.997487	0.997278	0.995268	0.997361

Table 3.14 Descriptive Statistics for the cross-correlation coefficients for stage 2

3.13.3 Stage 3

The box plot of the results from segments classified as stage 3 are seen in figure 3.15. Stage 3, or slow wave sleep is a very deep stage of sleep.[1] While in stage three, growth hormones are released, and immune system function occurs. Muscle tone is relaxed in the deeper stages of sleep.[1] This data can assist in determining if stage of sleep has an impact on the ability to detect respiration using movement. The descriptive statistics in for the stage 3 condition are found in Table 3.15.

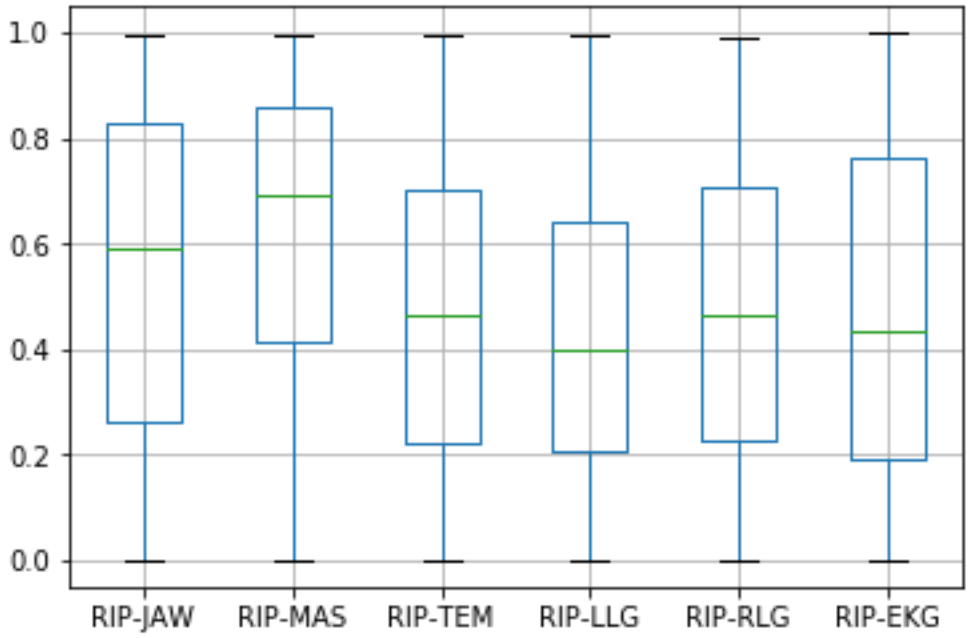

Figure 3.15 Boxplot of Stage 3 segments cross correlation coefficients

Table 3.15 Descriptive Statistics for the cross-correlation coefficients for stage 3

	Jawsens	Masseter	Temporalis	Left Leg	Right Leg	ECG
count	5991	5991	5991	5991	5991	5991
mean	0.546478	0.620695	0.467793	0.429196	0.469590	0.472263
std	0.303112	0.274727	0.277035	0.267391	0.275371	0.310183
min	0.000237	0.000150	0.000151	0.000066	0.000102	0.000070
25%	0.262582	0.414574	0.223972	0.204459	0.228553	0.194094
50%	0.588847	0.689922	0.466211	0.400603	0.465189	0.436397
75%	0.826096	0.857169	0.703879	0.639756	0.708304	0.762053
max	0.994888	0.993580	0.994760	0.996218	0.992463	0.998973

3.13.4 Stage REM

In stage REM, all muscles become paralyzed except the heart, diaphragm and eyes. It is also when obstructive respiratory events become more severe.[1] When the muscles relax, the airway is more easily blocked due to the loss of muscle tone. In this study, all the cross-correlation coefficients in the segments stages as REM are seen using a boxplot in figure 3.16.

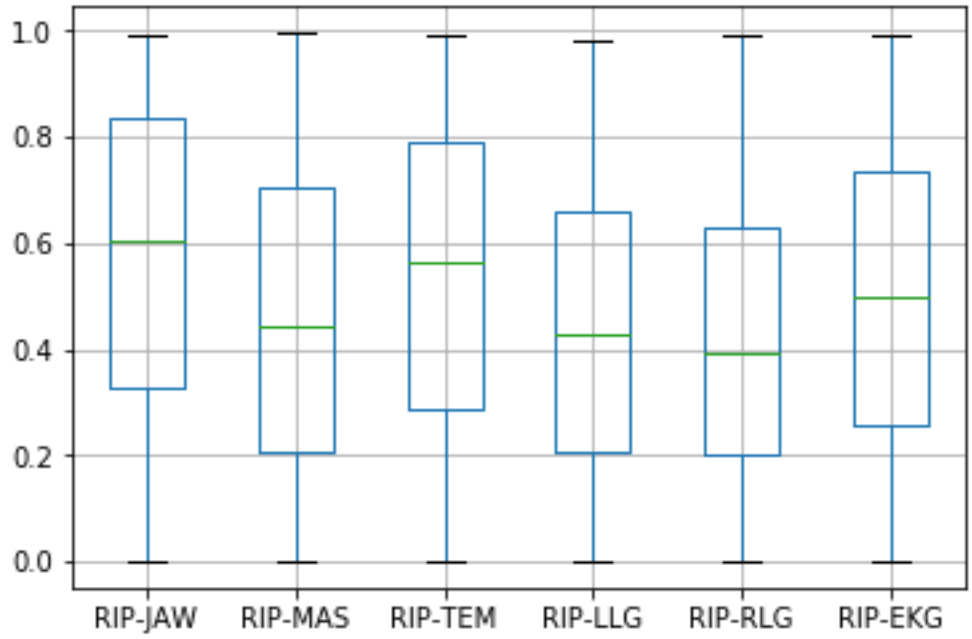

Figure 3.16 Boxplot of Stage REM segments cross correlation coefficients

The descriptive statistics from the dataset of all stage REM segments is found in table 3.16. The change in stage did seem to make a difference in the ability to detect respiratory effort using the various measures of movement. It is in this state that the Masseter correlated lower than all others and the lowest within its own abilities. This finding is consistent with our current understanding of changes in physiology in REM.

During inspiration, there are primary and secondary muscles and it is known that the elevation of the mandible is used to increase airway patency and this effect decreases in REM.[10]

Table 3.16 Descriptive Statistics for the cross-correlation coefficients for stage REM

	Jawsens	Masseter	Temporalis	Left Leg	Right Leg	ECG
count	3099	3099	3099	3099	3099	3099
mean	0.567075	0.459816	0.532784	0.433638	0.423752	0.492949
std	0.290904	0.288743	0.288457	0.266082	0.271787	0.276496
min	0.000285	0.000273	0.000282	0.000315	0.000233	0.000356
25%	0.326483	0.207920	0.286076	0.206536	0.200018	0.258213
50%	0.602377	0.441368	0.561404	0.427392	0.393831	0.499748
75%	0.835257	0.703817	0.790202	0.657982	0.628778	0.733932
max	0.992753	0.995538	0.993552	0.983266	0.991014	0.993819

3.13.5 Supine

The position during sleep does have a strong effect on respiration and does also increase the probability of upper airway collapse in someone who suffers from obstructive sleep apnea. The boxplot of the cross correlations from the segments labeled as supine is seen in figure 3.17.

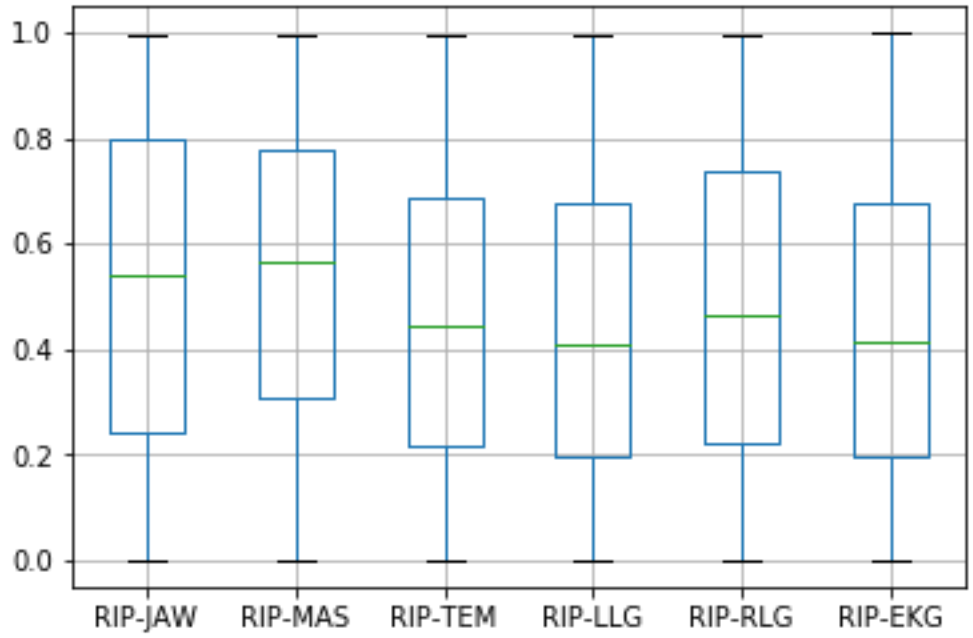

Figure 3.17 Boxplot of Supine position segments cross correlation coefficients

The descriptive statistics from the supine labeled segments is seen in table 3.17. Table 3.17 Descriptive Statistics for the cross-correlation coefficients for Supine position

	Jawsens	**Masseter**	**Temporalis**	**Left Leg**	**Right Leg**	**ECG**
count	13998	13998	13998	13998	13998	13998
mean	0.515996	0.536993	0.453382	0.443628	0.479559	0.440880
std	0.299499	0.276795	0.269792	0.288880	0.291408	0.282313
min	0.000057	0.000046	0.000052	0.000020	0.731283	0.000032
25%	0.239720	0.308394	0.218498	0.195065	0.222789	0.194284
50%	0.538803	0.564800	0.443935	0.408269	0.466016	0.412164
75%	0.795509	0.777985	0.684188	0.677182	0.738016	0.678483
max	0.993675	0.994207	0.996511	0.996218	9.931299e-01	0.998556

3.13.6 Non-Supine

The segments where positions were labeled left, or right were merged into a condition that will be considered non-supine. When a subject is on their side, the effects of gravity on the upper airway and is known to improve the ability to keep the airway open in those that suffer from obstructive sleep apnea.[1] The boxplot of this condition can be seen in figure 3.18.

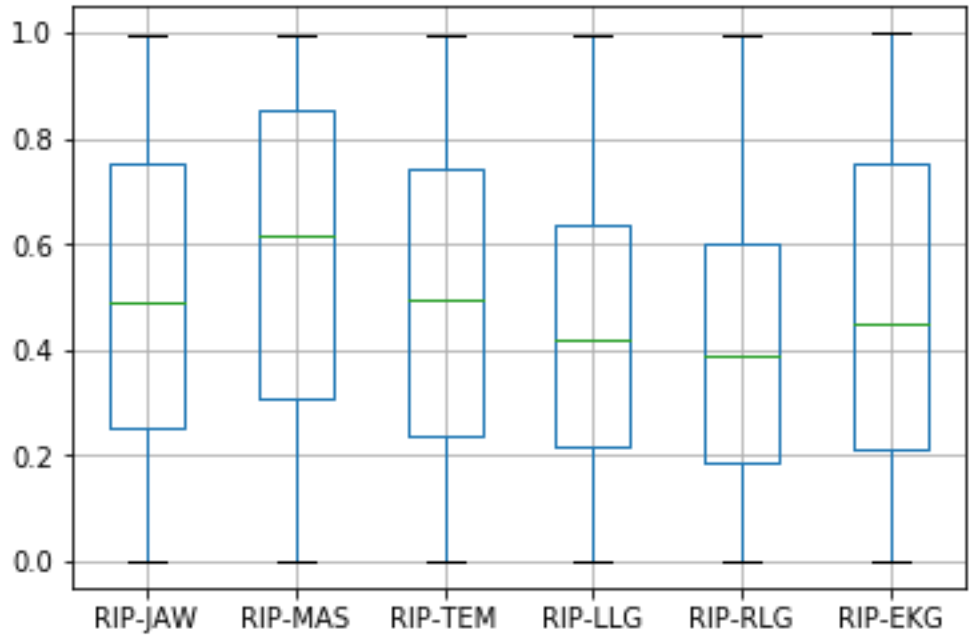

Figure 3.18 Boxplot of Non-Supine position segments cross correlation coefficients

The descriptive statistics for the non-supine condition is seen in table 3.18

Table 3.18 Descriptive Statistics for the cross-correlation coefficients for Non-Supine position

	Jawsens	Masseter	Temporalis	Left Leg	Right Leg	ECG
count	10338	10338	10338	10338	10338	10338
mean	0.497383	0.571246	0.492206	0.429740	0.406488	0.478146
std	0.287486	0.299888	0.289097	0.254909	0.255394	0.300818
min	0.000081	0.000150	0.000134	0.000132	0.000233	0.000104
25%	0.250570	0.310077	0.237638	0.215772	0.185726	0.210503
50%	0.491015	0.614606	0.495372	0.417119	0.387868	0.451241
75%	0.751931	0.852820	0.744795	0.638023	0.602112	0.754136
max	0.995876	0.996116	0.997487	0.997278	0.995269	0.998973

3.13.7 All States combined

All the previous data was combined into a single dataset to compare the ability of each sensor across all subjects and states. In figure 3.19, a box plot from all the cross-correlation coefficient calculations can be seen.

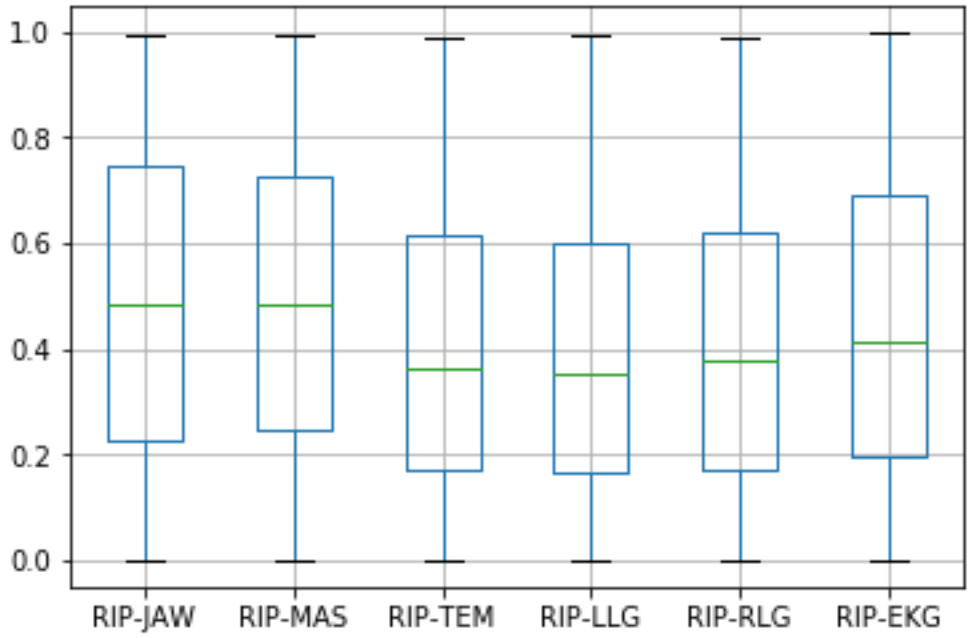

Figure 3.19 Boxplot of all sleep conditions

When comparing all of the available sensors, the Masseter produced the highest absolute cross correlation coefficient.

Table 3.19 Descriptive Statistics for the cross-correlation coefficients for All Sleep conditions

	Jawsens	Masseter	Temporalis	Left Leg	Right Leg	ECG
count	24344	24344	24344	24344	24344	24344
mean	0.508092	0.551539	0.469869	0.437730	0.448528	0.456705
std	0.294596	0.287322	0.278809	0.275047	0.279029	0.290893
min	0.000057	0.000046	0.000052	0.000020	0.731283	0.000032
25%	0.244624	0.308862	0.225935	0.203462	0.206363	0.200798
50%	0.518002	0.583679	0.464344	0.412111	0.427449	0.427771
75%	0.778510	0.810253	0.709374	0.659053	0.680401	0.709585
max	0.995876	0.996116	0.997487	0.997278	0.995268	0.998973

Chapter 4 – **Discussion**

In this chapter, the results will be interpreted technically and clinically. The limitations of the study will be discussed.

4.1 Clinical Interpretation

The data shows that in all twelve subjects, there is the ability to detect respiratory effort with the use of a motion artifact that comes from the filtered EMG and ECG data. There were four EMG sites and a ECG signal compared to the ability of the Jawsens device. In all states, the masseter performed better on average than the Jawsens except in stage REM sleep. The mechanism and explanation for why masseter muscle movement is related to respiratory effort may be why the magnetic jaw distance sensor also was able to detect respiratory effort. During inspiration the mouth has negative pressure applied to it causing a reduction in distance and the reverse occurs during exhalation. It is this mechanical force that is generated from the respiratory system that may be driving the movement that is seen that results in a signal that can match the signal from the belts.[10]

The mechanism for how caudal traction from inspiration may cause mandibular movements was observed to be from the pull of the descending diaphragm and the suction of increasingly negative intrathoracic pressure. This mechanism does explain how the mandibular movement can detect respiratory effort and how the Jawsens sensor operates.[10]

It has also been observed that the jaw stabilizes the airway in times of upper airway collapse and so that the jaw movements and EMG activity are measurements of the response to keep the airway open.[10]

The observation that the masseter's ability to detect respiration was reduced in REM was to be expected as all muscle activity is reduced in REM and the movement from the

masseter muscle is expected to be reduced and this was seen. This result also suggests that the signals from the distance sensor and the masseter after isolating the motion artifact are not exactly equivalent and that the sensors on the masseter are detecting movements that are impacted by muscle activity of the jaw elevator muscles and not only the diaphragmatic forces. In non-REM stages, these two effects are combined and give the masseter an advantage over the Jawsens which can only detect the mandibular movements. In the all sleep dataset, we observed that there was no difference in the overall ability for the movement artifact waveform to detect respiratory effort from that of the magnetic distance sensor.

It is also worthy of note that when the performance of the masseter sensor was reduced, the Jawsens increased. This may be related. In stage REM sleep, when the muscles are less active, the mandibular movements are greater due to the relaxation of the muscles keeping the mandible stable and so the Jawsens is better able to pick up the respiratory effort. The masseter has an airway stabilizing function that reduces in stage REM.

4.2 Technical Interpretation

The waveform obtained are the result of isolating the low frequency component of the EMG and ECG recordings. They are the result of movement and not direct electrical activity of the muscle or cardiac activity. The distance between the electrodes varies with movement which is the indirect the result of diaphragmatic excursions. It is this small deviation in distance that is seen as an increase in the amount of voltage measured with the EMG sensors. A similar mechanism is how respiratory effort was detected using the ECG. As the diaphragm descends, the ECG sensors move in synchrony and results in a waveform that can be used for respiratory effort.

The movement potentials are originating in a combination of the skin deformation and the movement of the conductive gel. These effects combine to produce the ability to detect movement using sensors intended for electrical activity measurements.[11] Due to the limited motions in sleep, most detectable movement will be the result of respiration and so a movement artifact waveform can be used as a detection of respiratory effort.

4.3 Performance

An average cross-correlation of 0.48 for the best motion artifact based may at first appear to be insignificant or not useful. The same value was obtained from the Jawsens signal and this device has been shown in multiple studies to be able to detect and classify respiratory events. The motion artifact recovered waveforms, having the same measured performance, are therefore as able to used in diagnosis. The performance of the method can also be increased by studying the methods for which motion artifact is generated and maximizing those parameters. Adjustments to the placement, electrode type, cable thickness can improve the amount of motion artifact detected and the performance of the method. This study shows the potential use of the method and can be used to generate further improvements in the future.

4.4 Study Limitations

The ability to measure respiratory effort in this study was measured against respiratory inductance plethysmography. The gold standard for the measurement is esophageal pressure manometry (PEs). A measure of PEs would be a valuable addition for validation of any measurement of respiratory effort. The availability and ability for a subject to tolerate Pes measurement is a challenge. It is invasive, uncomfortable and expensive.[3]

All the subjects in this study were diagnosed with obstructive sleep apnea. A study that includes healthy subjects should be performed to observe the possible affect that disordered breathing has on the correlation of effort with mandibular movements and movement artifact waveforms ability to detect respiration. It may be the case that the motion artifact effect observed is due to the need to keep the airway open due to closure in sleep in those individuals who have a tendency for airway collapse and we may see a different distribution of abilities in a healthy subject than those seen in this study.

Chapter 5 - **Conclusion**

In this chapter, the main findings and future directions will be discussed.

5.1 Main Findings

In this thesis, the need for the measurement of respiratory effort was discussed followed with the most common methods of obtaining the signal. It was observed that by smoothing electromyographic and electrocardiographic signals, a waveform that is the motion artifact of the signal results. The resulting waveform has been shown to correlate very well with the respiratory effort belt which uses inductance plethysmography as the method of detecting respiratory effort. There were six locations where this effect was measured. The masseter, temporalis, left and right anterior tibialis, and the electrocardiogram were all smoothed using the Savitzy-Golay method and then the cross-correlation coefficient was measured between the resulting waveform and the waveform from the RIP belt. The masseter did show the most promise as a location for which respiratory effort could be detected using this technique. There was a reduction in performance of this method while in stage REM, which was to be expected.

5.2 Future Directions

The ability of a single sensor to detect multiple signals is the goal of future diagnostics. Continued validation of this method is necessary before it can be recommended in use clinically. To better understand the mechanisms for this, variations to the placement of the electrodes should be made to see if increased performance is possible. Other signal processing techniques may also be attempted or developed to increase the performance of the technique.

References

1. Rachel E. Salas, Rohini Chakravarthy, Alex Sher, Charlene E. Gamaldo. *Management of sleep apnea in the neurology patient*. Neurol Clin Pract Feb 2014, 4 (1) 44-52;
2. Berry RB, Brooks R, Gamaldo CE., "The AASM manual for the scoring of sleep and associated events: rules, terminology and technical specifications, Version 2.2." www.aasmnet.org. Darien, IL: American Academy of Sleep Medicine, 2015
3. Vandenbussche NL, Overeem S, van Dijk JP, Simons PJ, Pevernagie DA, authors. *Assessment of respiratory effort during sleep: esophageal pressure versus noninvasive monitoring techniques.* Sleep Med Rev. 2015;24:28–36.
4. Senny F, Destine J, Poirrier R. *Midsagittal jaw movement analysis for the scoring of sleep apneas and hypopneas.* IEEE Trans Biomed Eng 2008 Jan;55(1):87e95.
5. Sabaneeff, Ana, Caldas, Luciana Duarte, Garcia, Marco Antonio Cavalcanti, & Nojima, Matilde da Cunha Gonçalves. *Proposal of surface electromyography signal acquisition protocols for masseter and temporalis muscles.* Research on Biomedical Engineering, (2017), 33(4), 324-330.
6. Gramfort, M. Luessi, E. Larson, D. Engemann, D. Strohmeier, C. Brodbeck, L. Parkkonen, M. Hämäläinen, MNE software for processing MEG and EEG data, NeuroImage, Volume 86, 1 February 2014, Pages 446-460, ISSN 1053-8119
7. Gramfort, M. Luessi, E. Larson, D. Engemann, D. Strohmeier, C. Brodbeck, R. Goj, M. Jas, T. Brooks, L. Parkkonen, M. Hämäläinen, MEG and EEG data analysis with MNE-Python, Frontiers in Neuroscience, Volume 7, 2013, ISSN 1662-453X
8. A. Savitzky, M. J. E. Golay. Soothing and differentiation of data by simplified least squares procedures. Anal. Chem. 1964. vol. 36, pp. 1627-1639,

9. R.W. Schafer. What is a Savitzky–Golay filter?. IEEE Signal Process. Mag., vol. 28, no. 4, pp. 111-117, 2011.
10. Van de Graaff WB. Thoracic influence on upper airway patency. J Appl Physiol (1985). 1988;65(5):2124–31.
11. Ödman, S. & Åke Öberg, Movement-induced potentials in surface electrodes P. Med. Biol. Eng. Comput. (1982) 20: 159.